REPORT DOCUMENTATION PAGE

AFRL-SR-AR-TR-04-

0561

1. REPORT DATE *(DD-MM-YYYY)*	2. REPORT TYPE	3. DATES COVERED *(From - To)*
	Final Report	1 Apr 2003 - 30 Jun 2004

4. TITLE AND SUBTITLE
Uncertainties and Relaxation of Boundary Conditions of Aereoelastic Panels

5a. CONTRACT NUMBER

5b. GRANT NUMBER
F49620-03-1-0229
~~F496220-03-1-0229~~

5c. PROGRAM ELEMENT NUMBER

6. AUTHOR(S)
Dr. Raouf A. Ibrahim

5d. PROJECT NUMBER

5e. TASK NUMBER

5f. WORK UNIT NUMBER

7. PERFORMING ORGANIZATION NAME(S) AND ADDRESS(ES)
Department of Mechanical Engineering
Wayne State University
Detroit MI 48202

8. PERFORMING ORGANIZATION REPORT NUMBER

9. SPONSORING/MONITORING AGENCY NAME(S) AND ADDRESS(ES)
USAF/AFRL
AFOSR
801 N. Randolph Street
Arlington VA 22203
NA

10. SPONSOR/MONITOR'S ACRONYM(S)
AFOSR

11. SPONSOR/MONITOR'S REPORT NUMBER(S)

12. DISTRIBUTION/AVAILABILITY STATEMENT

Distribution Statement A. Approved for publiic release; distribution is unlimited.

13. SUPPLEMENTARY NOTES

20041112 035

14. ABSTRACT

The influence of boundary condition relaxation on two-dimensional panel flutter is studied in the presence of in-plane loading. The boundary value problem of the panel involves time-dependent boundary conditions that are converted into autonomous form using a special coordinate transformation. Galerkin's method is used to discretize the panel partial differential equation into six nonlinear ordinary differential equations representing the first six modes. The influence of boundary condition relaxation on the panel modal frequencies and limit cycle amplitudes in the time and frequency domains is examined through the spectrogram of the generalized coordinate for each mode. The relaxation and system nonlinearity are found to have opposite effects on the time evolution of the panel frequency. Depending on the system damping and dynamic pressure, the panel frequency content can increase or decrease with time as the boundary conditions approach simple supports. Bifurcation diagrams are generated by taking the dynamic pressure and relaxation parameter as control parameters. They reveal different regions of periodic, quasi-periodic, and chaotic motions. These regions take place only when the in-plane load exceeds the Euler buckling load.

15. SUBJECT TERMS

16. SECURITY CLASSIFICATION OF:			17. LIMITATION OF ABSTRACT	18. NUMBER OF PAGES	19a. NAME OF RESPONSIBLE PERSON
a. REPORT	b. ABSTRACT	c. THIS PAGE			19b. TELEPHONE NUMBER *(Include area code)*
U	U	U	UU	33	

Final Report

Project Title: Uncertainties and Relaxation of Boundary Conditions of Aereoelastic Panels

AFOSR Grant No. ~~FA9620-03-0229~~ F49620-03-1-0229

Duration: April 1, 2003 to June 30, 2004 (including no-cost extension for 6 months)

P.I.: Raouf A. Ibrahim
Department of Mechanical Engineering
Wayne State University
Detroit, MI 48202
Tel. (313) 577-3885
Fax (313) 577-8789
e.mail: ibrahim@eng.wayne.edu

Students Supervised: Mr. D. M. Beloiu, Ph.D.

Publications, Presentations

1. Ibrahim, R. A., Beloiu, D. M., and Pettit, C. L., 2004, "Influence of Joint Relaxation on Deterministic and Stochastic Panel Flutter," *AIAA Journal*, in press.
2. Ibrahim, R. A., Beloiu, D. M., and Pettit, C. L., 2003, "Influence of Boundary Conditions Relaxation on Panel Flutter," IUTAM Symposium on Chaotic Dynamics and Control of Systems and Processes in Mechanics, Rome, Italy, 8-13 June 2003.
3. Ibrahim, R. A. Beloiu, D.M and Pettit, C. L., 2003, "Influence on Boundary Conditions Relaxation on Panel Flutter: Deterministic and Stochastic," AFOSR Workshop Contractors Meeting, Santa Fe, New Mexico, September 8-112, 3003.
4. Ibrahim, R. A. Beloiu, D.M and Pettit, C. L., 2004, "Influence of Joint Relaxation on Deterministic and Stochastic Panel Flutter," Flow Induced Vibration, de Langre & Axisa ed., Ecole Polytechnique, Paris, July 6-9.
5. Ibrahim, R. A. Beloiu, D.M and Pettit, C. L., 2004, "Influence of Boundary Conditions Relaxation on Panel Flutter with in-Plane Loads," AFOSR Workshop Contractors Meeting, Winter Green, VA, August 18-20.
6. Beloiu, D.M, Ibrahim, R. A., and Pettit, C. L.,??, "Influence of Boundary Conditions Relaxation on Panel Flutter with Compressive in-Plane Loads," Submitted for possible publication to the *Journal of Fluids and Structures*.
7. Ibrahim, R. A. Beloiu, D.M and Pettit, C. L., 2004, "Six-Mode Interaction of Panel Flutter with Joint Relaxation: Deterministic Analysis," Proc IMECE2004, 2004 ASME International Mechanical Engineering Congress and RD&D Expo November 13-19, 2004, Anaheim, California USA.

SIX-MODE INTERACTION OF PANEL FLUTTER WITH JOINT RELAXATION
PART I: DETERMINISTIC ANALYSIS

R. A. Ibrahim, D. M. Beloiu
Wayne State University
Department of Mechanical Engineering
Detroit, MI 48202

C. L. Pettit
Air Force Research Laboratory
AFRL/VASD
Wright-Patterson Air Force Base, OH 45433

ABSTRACT

The influence of boundary condition relaxation on two-dimensional panel flutter is studied in the presence of in-plane loading. The boundary value problem of the panel involves time-dependent boundary conditions that are converted into autonomous form using a special coordinate transformation. Galerkin's method is used to discretize the panel partial differential equation into six nonlinear ordinary differential equations representing the first six modes. The influence of boundary condition relaxation on the panel modal frequencies and limit cycle amplitudes in the time and frequency domains is examined through the spectrogram of the generalized coordinate for each mode. The relaxation and system nonlinearity are found to have opposite effects on the time evolution of the panel frequency. Depending on the system damping and dynamic pressure, the panel frequency content can increase or decrease with time as the boundary conditions approach simple supports. Bifurcation diagrams are generated by taking the dynamic pressure and relaxation parameter as control parameters. They reveal different regions of periodic, quasi-periodic, and chaotic motions. These regions take place only when the in-plane load exceeds the Euler buckling load.

I. INTRODUCTION

It has been observed that apparently identical aircraft can exhibit different dynamic characteristics under same flight conditions. This difference owes its origin to the stochastic nature of structural properties and the environment. That is, the sensitivity of the dynamic system behavior is directly linked to variations in its physical properties; in aeroelastic systems, response variability is compounded by interaction with the surrounding fluid. The physical properties of aeroelastic structures are affected by the boundary conditions relaxation and joint uncertainties. Generally, the main sources of uncertainties of aerospace structures include:

1. Randomness in material properties because of variations in material composition.
2. Randomness in structural dimensions due to manufacturing variations and thermal effects.
3. Randomness in boundary conditions due to preload and relaxation variations in mechanical joints.
4. Randomness of external excitations.

The present work is focused on the third source and its mechanisms. There are many factors that affect mechanical joints and fasteners, such as friction, hardness, finish, and dimensions of all parts, and gasket creep (Bickford, 1990). Each factor will vary from fastener to fastener and joint to joint because of manufacturing or usage tolerances. A fastener subjected to vibration will not lose all pre-loads immediately. First there is a slow loss of pre-load caused by various relaxation mechanisms. Vibration increases relaxation through the consequent wear and hammering. After sufficient pre-load is lost, friction forces drop below a critical level and, if the joint is bolted, the nut actually starts to back off and shake loose. As relaxation occurs, the joint fails to mimic ideal boundary conditions; instead, the joint's properties become time dependent and uncertain.

The present work is motivated by some recent results on the sensitivity and variability of the response of structural stochasticity (see, for example, Ibrahim, 1987, and Manohar and Ibrahim, 1999) and by the recent assessment of joint uncertainties by Ibrahim and

Pettit (2004). These problems are complex in nature because every joint involves different sources of uncertainty and non-smooth nonlinear characteristics. For example, the contact forces are not ideally plane because of manufacturing tolerances. Furthermore, the initial forces will be redistributed non-uniformly in the presence of lateral loads. This is in addition to the prying load, which induces nonlinear tension in the bolt and nonlinear compression in the joint. The main problems encountered in the design analysis of bolted joints with parameter uncertainties include random eigenvalues, response statistics, and probability of failure.

The effect of uncertainty in the boundary conditions combined with the variability of material properties on nonlinear panel aeroelastic response was studied by Lindsley, et al. (2002a, b). It was shown that the flutter problem of aeroelastic structures could be handled when random uncertainties are introduced in the structural model. The pinned and fixed boundary conditions were modeled as limiting cases of rotational springs on the boundary, which possess zero and infinite stiffness, respectively. Accordingly, rotational spring stiffness was used to parameterize the boundary conditions. Parametric uncertainty was examined by modeling variability in Young's modulus and the boundary condition parameter. The variability in the boundary conditions was restricted to a single value along the plate boundary edges for each realization. For values of the dynamic pressure in the deterministic limit cycle oscillation (LCO) range, the variability in the boundary conditions affects the plate deflection in an essentially linear manner. However, for values of dynamic pressure in the neighborhood of bifurcation point, the relationship is nonlinear. Variation in boundary conditions results in a softening effect of the clamped panel, and thus induces an increase in the amplitude of plate oscillations.

Relaxation effects cause time-dependent boundary conditions and depend on the level of structural vibration. In other words, there are uncertainties in the boundary conditions in addition to a random field due to system parameter uncertainties. Under static loads, the design of such systems is governed by the random field alone, whereas under dynamic loads, the designer also must take into account the temporal fluctuations of the boundary conditions. During operation, the nonlinear random response can generally change a joint's mechanical properties and hence create new self-induced uncertainties.

The studies of panel flutter were concentrated on parametric analysis of the stability boundaries and the amplitude of limit cycle oscillations under different boundary conditions. At the same time, it was shown that a panel subjected to a combination of airflow and in-plane loading experiences a complex range of motions, including static buckling (divergence), quasi-periodic motion, and chaos in addition to limit cycle oscillations. Dowell (1982) showed that a panel under the combined effect of fluid flow and in-plane compression exhibits chaotic motion for certain values of some control parameters. Dowell (1984) observed chaos via period doubling and intermittency while increasing the compressive in-plane loading. The existence of multiple attractors and the coexistence of both symmetric and asymmetric limit cycles were observed by Bolotin et al. (1998) using a two degree-of-freedom approximation of an elastic panel. They studied the transition between different stability regions. The stability regions of a simply supported two-dimensional panel subjected to compressive loading were revisited recently by Epureanu et al. (2004). They used bifurcation diagrams for two control parameters to determine stability boundaries and Lyapunov exponents. The effect of damping on stability boundaries as well as on LCO was considered by Kuo et al. (1972), Bolotin et al. (2002), Pourtakdoust and Fazelzadeh (2003). Kuo et al. (1972) showed that the edge compression and viscous structural damping increases flutter amplitudes while the aerodynamic damping decreases flutter amplitude.

In this paper, nonlinear panel flutter with relaxation in the boundary conditions is studied based on a phenomenological model of joint preload relaxation pressure superposed on linear piston theory loads. The conventional boundary value problem of the panel involves time-dependent boundary conditions, which are converted to an autonomous form using a special coordinate transformation inspired by the work of Qiao, et al. (2000). It has been claimed (Dowell, 1966) that accurate results of panel flutter are obtained by considering at least six-mode interaction. The present analysis extends the analysis of Ibrahim, et al. (2004) to include six-mode interaction in the presence of boundary condition relaxation.

II. ANALYTICAL MODELING

Consider a two dimensional panel exposed to supersonic flow as shown in Figure 1. In order to estimate the work done by aerodynamic loading, the pressure on the panel is estimated using the linear piston theory (Ashley and Zartarian, 1956)

$$\Delta p = p - p_\infty = \frac{\rho_\infty U_\infty^2}{M}\left[\frac{\partial w}{\partial x} + \frac{1}{U_\infty}\frac{\partial w}{\partial t}\right] \tag{1}$$

where $w(x,t)$ is the panel deflection, which is a function of position, x, and time, t, $M = U_\infty / a_\infty$ is the Mach number, U_∞ is the undisturbed gas flow speed, $a_\infty = \sqrt{\gamma p_\infty / \rho_\infty}$ is the speed of sound, p_∞ and ρ_∞ are the undisturbed free gas stream pressure and density, respectively, p is the pressure of the gas flow at the panel surface, $\gamma = C_p / C_v$ is the ratio of specific heat at constant pressure, C_p, and volume, C_v.

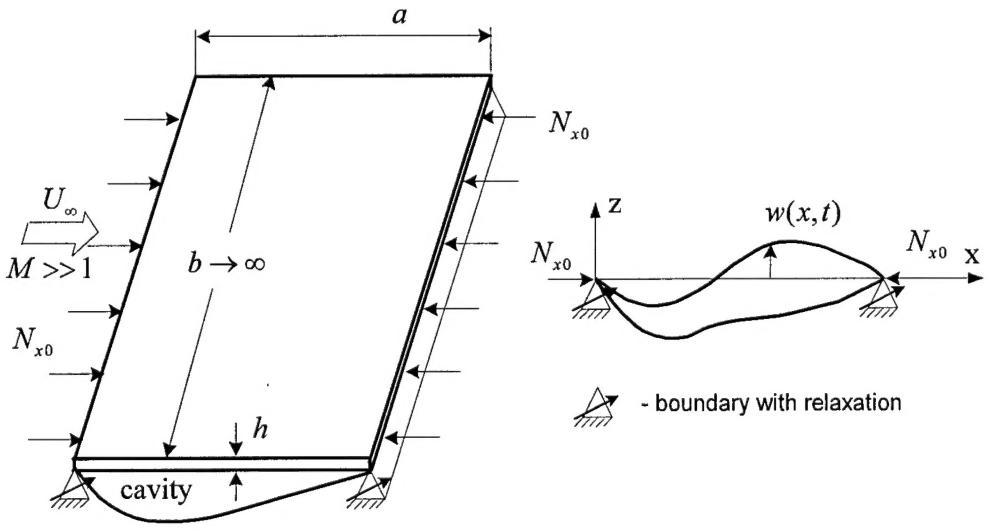

Figure 1. Schematic diagram of a two-dimensional panel with boundary conditions relaxation

The governing nonlinear equation of motion for the panel is developed using Hamilton's principle, which yields (Ibrahim, et al., 1990)

$$m_p \frac{\partial^2 w}{\partial t^2} + D\left(1 + c\frac{\partial}{\partial t}\right)\frac{\partial^4 w}{\partial x^4} - \left[N_{x0} + \frac{Eh}{2a}\int_0^a \left(\frac{\partial w}{\partial x}\right)^2 dx\right]\frac{\partial^2 w}{\partial x^2} +$$

$$+ \frac{\rho_\infty U_\infty^2}{M}\left[\frac{\partial w}{\partial x} + \frac{1}{U_\infty}\frac{\partial w}{\partial t}\right] = \Delta p_0 \qquad (2)$$

m_p is the panel mass per unit area, a is the panel length, E is Young's modulus, h is the plate thickness, $D = Eh^3/(12(1-\nu^2))$ is the panel stiffness, ν is Poisson's ratio, Δp_0 is the air pressure difference across the panel, N_{x0} is the external in-plane load per unit span-wise length, and c is a linear viscous damping coefficient. Equation (2) is subject to the boundary conditions

$$D\frac{\partial^2 w(0,t)}{\partial x^2} - \alpha_1(t)\frac{\partial w(0,t)}{\partial x} = 0, \qquad w(0,t) = 0 \qquad (3a,b)$$

$$D\frac{\partial^2 w(a,t)}{\partial x^2} + \alpha_2(t)\frac{\partial w(a,t)}{\partial x} = 0, \qquad w(a,t) = 0 \qquad (3c,d)$$

where $\alpha_1(t)$ and $\alpha_2(t)$ measure the end slopes and represent torsional stiffness parameters such that for $\alpha_1(t) = \alpha_2(t) = \infty$ we have the case of purely clamped-clamped panel. On the other hand, if we have simple supports, then $\alpha_1(t) = \alpha_2(t) = 0$. In real situations, $\alpha_1(t)$ and $\alpha_2(t)$ do not assume these limiting cases; instead, they are very large for clamped supports or very small for simple supports. In the dynamic case the boundary conditions (3a,c) are non-autonomous. In order to convert these conditions into an autonomous form, we introduce the following transformation of the response coordinate,

$$w(x,t) = \left[\left(\frac{x}{a}\right)^2 + 2g_1(z_1,z_2)\frac{x}{a} + g_2(z_1,z_2)\right]u(x,t) = \varphi(x;z_1,z_2)u(x,t) \qquad (4)$$

where the dimensionless parameter $z_i(t) = D/a\alpha_i(t)$, $i = 1,2$, represents the ratio of the bending rigidity to the torsional stiffness of the joints. The functions $g_1(z_1,z_2)$ and

$g_2(z_1, z_2)$ are chosen to render the boundary conditions autonomous for the new coordinate $u(x,t)$. Possible expressions of these functions are

$$g_1(z_1, z_2) = -\frac{1+4z_2}{2(1+2z_1+2z_2)} \qquad g_2(z_1, z_2) = -\frac{2z_1(1+4z_2)}{1+2z_1+2z_2} \tag{5}$$

In this case, the boundary conditions (3) become

$$\frac{\partial^2 u(0,t)}{\partial x^2} = \frac{\partial^2 u(a,t)}{\partial x^2} = 0 \qquad \text{and } u(0,t) = u(a,t) = 0. \tag{6}$$

Introducing the following non-dimensional parameters

$$\tau = t\sqrt{\frac{D}{m_p a^4}};\ \bar{w} = \frac{w}{h};\ \bar{x} = \frac{x}{a};\ \lambda = \frac{\rho_\infty U_\infty^2 a^3}{MD};\ \mu = \frac{\rho_\infty a}{m_p};\ \zeta = \frac{c}{a^2}\sqrt{\frac{D}{m_p}};$$

$$\bar{N}_0 = N_{x0}\frac{a^2}{D};\ \bar{p}_0 = \Delta p_0 \frac{a^4}{Dh};\ B_1 = 6(1-\nu^2);\ \ \bar{u} = \frac{u}{h};$$

$$\bar{\varphi} = \left[\bar{x}^2 + 2g_1(z_1, z_2)\bar{x} + g_2(z_1, z_2)\right];\ \hat{\zeta} = \sqrt{\frac{\mu}{M}}$$

equation (2) becomes

$$\frac{\partial^2(\bar{\varphi}\bar{u})}{\partial\tau^2} + \left(1 + \zeta\frac{\partial}{\partial\tau}\right)\frac{\partial^4(\bar{\varphi}\bar{u})}{\partial\bar{x}^4} - \left[\bar{N}_0 + B_1\int_0^1\left(\frac{\partial(\bar{\varphi}\bar{u})}{\partial\bar{x}}\right)^2 d\bar{x}\right]\frac{\partial^2(\bar{\varphi}\bar{u})}{\partial\bar{x}^2} +$$

$$+\lambda\frac{\partial(\bar{\varphi}\bar{u})}{\partial\bar{x}} + \hat{\zeta}\sqrt{\lambda}\frac{\partial(\bar{\varphi}\bar{u})}{\partial\tau} = \bar{p}_0 \tag{7}$$

The preload relaxation process is phenomenologically modeled based on experimental results. In this case, The torsional stiffness parameters are assumed functions of the number of vibration cycles (Bickford, 1990), $n = n(\tau)$,

$$\bar{\alpha}_i(n) = \frac{a\alpha_i(n)}{D} = \frac{1}{z_i(n)} \tag{8}$$

where the overbar denotes a dimensionless parameter. An explicit analytical expression for the parameters $\bar{\alpha}_i(n)$ can be obtained from experimental records (Bickford, 1990), which reveal a slow drop between an original and an asymptotic value of the joint

stiffness. An appropriate elementary function that emulates this behavior may be selected in the form

$$\bar{\alpha}(n) = \bar{\alpha}(\infty) + [\bar{\alpha}(0) - \bar{\alpha}(\infty)]\left[\frac{1+\tanh[-k(n-n_c)]}{1+\tanh[kn_c]}\right] \tag{9}$$

where the subscript i has been dropped, and n_c is a critical number of cycles, indicating the location of the inflection point with respect to the origin, $n = 0$. The parameter k is associated with the slope of the curve at the point, $n = n_c$. The parameters $\bar{\alpha}(0)$ and $\bar{\alpha}(\infty)$ are obtained from the experimental curve. The slope parameter k can be found by taking the derivative of equation (9) with respect to n, i.e.,

$$k = \frac{\partial \bar{\alpha}(n)/\partial n\big|_{n_c}}{[\bar{\alpha}(\infty) - \bar{\alpha}(0)]}[1+\tanh[kn_c]] \tag{10}$$

One can write an expression for $z(\tau)$ by using relations (8) and (10) in the form

$$z(\tau) = Z_0 Z_\infty \left[Z_0 - (Z_0 - Z_\infty)\frac{1+\tanh(-\chi(\tau-\tau_c))}{1+\tanh(\chi\tau_c)}\right]^{-1} \tag{11}$$

where $Z_0 = z(0)$, $Z_\infty = z(\infty)$, $\chi = \dfrac{<\varpi>}{2\pi k}$, and $<\varpi>$ is the mean value of the response frequency, which can be taken as the center frequency. The phenomenological representation given by equation (11) can be used for any initial preload and will cause the panel to experience non-stationary behavior.

Galerkin's method is applied to discretize equation (7) by assuming the general solution in the form $\bar{u}(\bar{x},\tau) = \sum_{n=1}^{N} \Psi_n(\bar{x}) q_n(\tau)$ and the corresponding weighting functions $\tilde{u}(\bar{x},\tau) = \sum_{n=1}^{N} \Psi_n(\bar{x}) \tilde{q}_n(\tau)$ where N is the total number of the basis functions for $\bar{u}(\bar{x},\tau)$; $q_n(\tau)$ are unknown functions to be determined (generalized coordinates); $\tilde{q}_n(\tau)$ are arbitrary functions of time and $\Psi_n(\bar{x})$ are the assumed orthonormal mode shapes. The resulting general differential equation is

$$\sum_{n=1}^{N} q_n''(\tau)\delta_{nm} + \sum_{n=1}^{N} q_n(\tau)C_1(n,m) + \zeta\sum_{n=1}^{N} q_n'(\tau)C_1(n,m) - \sum_{n=1}^{N} q_n(\tau)\bar{N}_{x0}C_2(n,m) -$$

$$-B_1\sum_{n=1}^{N} q_n(\tau)C_2(n,m)\left(\int_0^1\left(\sum_{n=1}^{N} q_k(\tau)(\varphi'(\bar{x})\Psi_k(\bar{x}) + \varphi(\bar{x})\Psi_k'(\bar{x})\right)^2 d\bar{x}\right) +$$

$$+\sum_{n=1}^{N} q_n(\tau)D_1(n,m) + \lambda\sum_{n=1}^{N} q_n(\tau)D_2(n,m) + \hat{\zeta}\sqrt{\lambda}\sum_{n=1}^{N} q_n'(\tau)D_3(n,m) = \bar{p}_0 D_4(m) \qquad (12)$$

where

$$\delta_{nm} = \int_0^1 \varphi(\bar{x})\Psi_n(\bar{x})\Psi_m(\bar{x})d\bar{x};$$

$$C_1(n,m) = 6\int_0^1 \varphi''(\bar{x})\Psi_n''(\bar{x})\Psi_m(\bar{x})d\bar{x} + 4\int_0^1 \varphi^{(3)}(\bar{x})\Psi_n'(\bar{x})\Psi_m(\bar{x})d\bar{x} +$$

$$+4\int_0^1 \varphi'(\bar{x})\Psi_n^{(3)}(\bar{x})\Psi_m(\bar{x})d\bar{x} + \int_0^1 \varphi^{(4)}(\bar{x})\Psi_n(\bar{x})\Psi_m(\bar{x})d\bar{x} + \int_0^1 \varphi(\bar{x})\Psi_n^{(4)}(\bar{x})\Psi_m(\bar{x})d\bar{x};$$

$$C_2(n,m) = 6\int_0^1 \varphi''(\bar{x})\Psi_n(\bar{x})\Psi_m(\bar{x})d\bar{x} + 2\int_0^1 \varphi'(\bar{x})\Psi_n'(\bar{x})\Psi_m(\bar{x})d\bar{x} + 6\int_0^1 \varphi(\bar{x})\Psi_n''(\bar{x})\Psi_m(\bar{x})d\bar{x};$$

$$D_1(n,m) = \int_0^1 \varphi'(\bar{x})\Psi_n(\bar{x})\Psi_m(\bar{x})d\bar{x};\ D_2(n,m) = \int_0^1 \varphi(\bar{x})\Psi_n'(\bar{x})\Psi_m(\bar{x})d\bar{x};\ D_3(n,m) = \delta_{nm};$$

$$D_4(m) = \int_0^1 \Psi_m(\bar{x})d\bar{x}.$$

The general solution is assumed in the form

$$\bar{u}(\bar{x},\tau) = \sum_{n=1}^{N} q_n(\tau)\sin n\pi\bar{x} \qquad (13)$$

where N is the total number of modes, $q_n(\tau)$ are the generalized coordinates. It has been established that accurate solution of the panel flutter can be achieved by using at least six modes (see, e.g., Dowell, 1966). The inclusion of six modes results in more tedious analysis and for this reason we introduce the simplification, $z_1 = z_2 = z/2$, which makes

the boundary stiffness values to be equal. The resulting set of six equations may be written in matrix form

$$[M(\tau)]\{\ddot{q}\}+\left[C(\zeta,\hat{\zeta},\lambda,\tau)\right]\{\dot{q}\}+\left[K(\tau,\bar{N}_0,\lambda)\right]\{q\}=[D(\tau)]\{q^3\}+\sum_{i=1,3,5}^{6}\sum_{j=1,j\neq i}\{eq_iq_j^2\}+$$
$$+\sum_{i}^{i\neq j\neq k}\sum_{j}\sum_{k}\{fq_iq_jq_k\}+\{\mathbf{P}\} \qquad (14)$$

where $[M(\tau)]$ is time dependent mass matrix; $\left[C(\zeta,\hat{\zeta},\lambda,\tau)\right]$ is the damping matrix, which depends on the viscous damping ratio ζ, mass parameter, $\hat{\zeta}$, and relaxation parameter, $z(\tau)$; $\left[K(\tau,\bar{N}_0,\lambda)\right]$ is the stiffness matrix; $[D(\tau)]$ is the coefficient matrix of cubic terms, and $\{P\}$ is the pressure vector, whose elements are non-zero only for odd modes. The structure of these matrices is given in the Appendix.

Equations (14) are solved numerically in the time domain for a typical relaxation curve. The resulting solution is given in terms of the transformed response, $\bar{u}$, or rather in terms of its modal coordinates, q_i, $i=1..6$. One should estimate the modal response in terms of its physical generalized coordinate,

$$\bar{w}(\bar{x},\tau)=\varphi(\bar{x})\bar{u}(\bar{x},\tau) \quad \text{and} \quad \bar{w}(\bar{x},\tau)=\sum_{n=1}^{N}\hat{q}_n(\tau)\sin n\pi\bar{x} \qquad (15)$$

where $\bar{\varphi}=\left[\bar{x}^2+2g_1(z_1,z_2)\bar{x}+g_2(z_1,z_2)\right]$ and g_i are given by equation (5). The relationship between the physical coordinates $\hat{q}_n(\tau)$ and the generalized transformed coordinates $q_n(\tau)$ is

$$\sum_{n=1}^{N}\hat{q}_n(\tau)\sin n\pi\bar{x}=\left[\bar{x}^2+2g_1(z)\bar{x}+g_2(z)\right]\sum_{n=1}^{N}q_n(\tau)\sin n\pi\bar{x} \qquad (16)$$

Integrating the above equation

$$\int_0^1\left[\sum_{n=1}^{N}\hat{q}_n(\tau)\sin n\pi\bar{x}\right]dx=\int_0^1\left[\left(\bar{x}^2+2g_1(z)\bar{x}+g_2(z)\right)\sum_{n=1}^{N}q_n(\tau)\sin n\pi\bar{x}\right]dx$$

gives the desired relation between the coordinates.

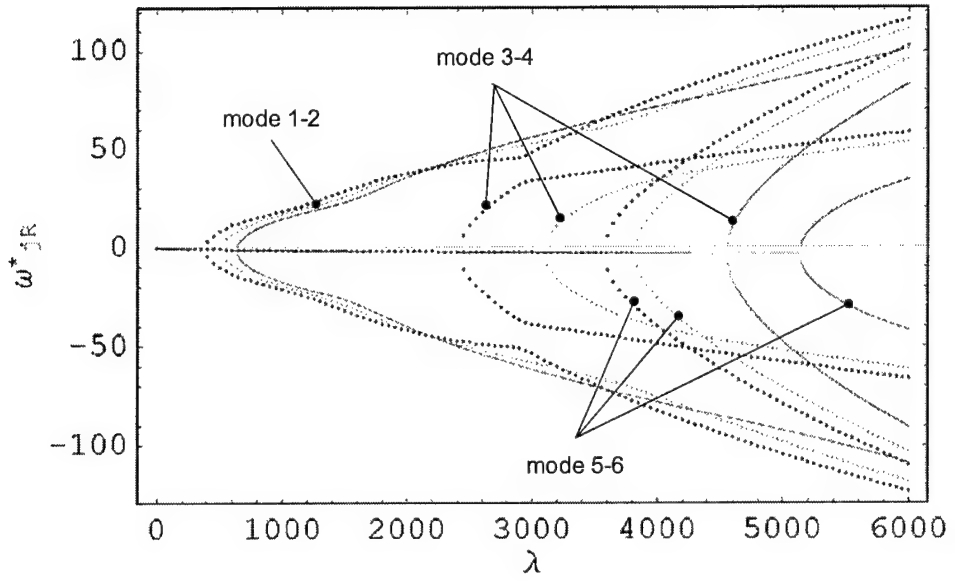

(a)

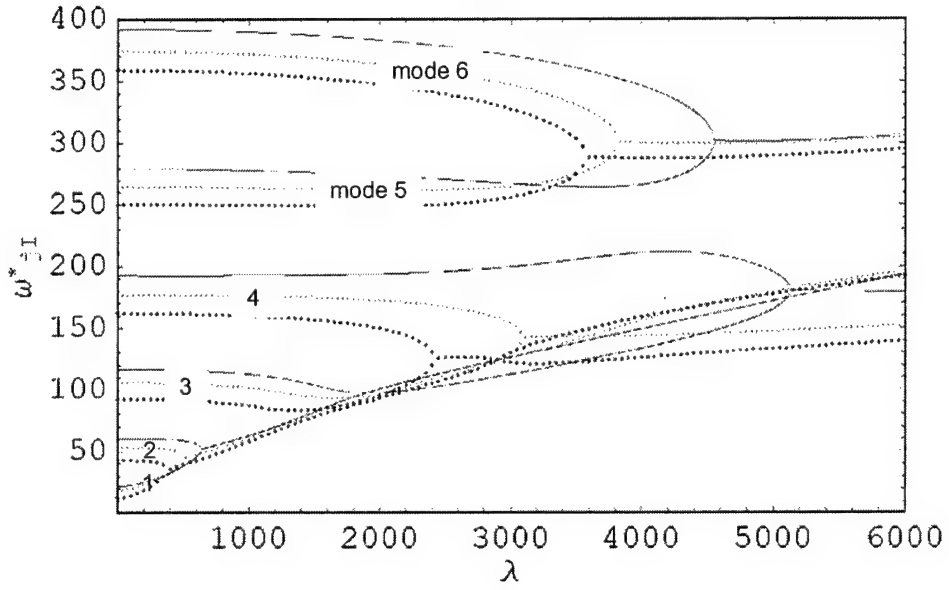

(b)

Figure 2. Dependence of real and imaginary parts of the panel natural frequency on dynamic pressure for $\zeta = 0; \hat{\zeta} = 0.1; \bar{N}_0 = 0$ (a) real parts, (b) imaginary parts. —z=0.001; ····· z=0.1; ····· z=1;

$$\hat{q}_n(\tau) = T_n(z) q_n(\tau) \tag{17}$$

where

$$T_n(z) = -\frac{(2n-1)^2\pi^2}{2+(2n-1)^2\pi^2 z}, \text{ n=1,3,5,...,} \qquad T_n(z) = -\frac{(n-1)^2\pi^2}{2+(n-1)^2\pi^2 z}, \text{ n=2,4,6,...} \tag{18}$$

Therefore, the solution of equations (14) must be divided by $T_n(z)$ in order to recover the actual modal displacements. The next section presents the stability analysis and response characteristics under different values of dynamic pressure and relaxation parameter.

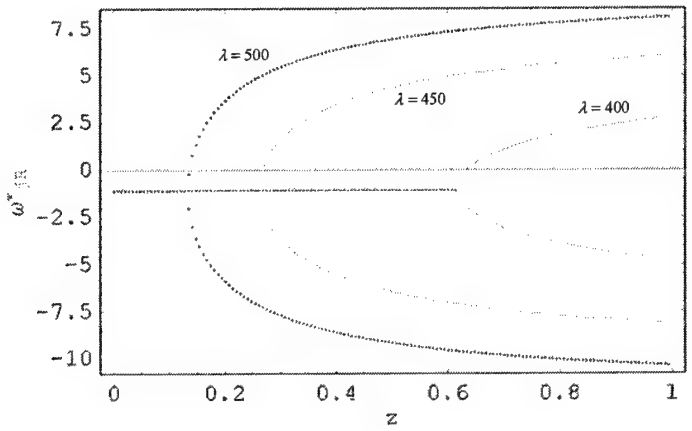

(a)

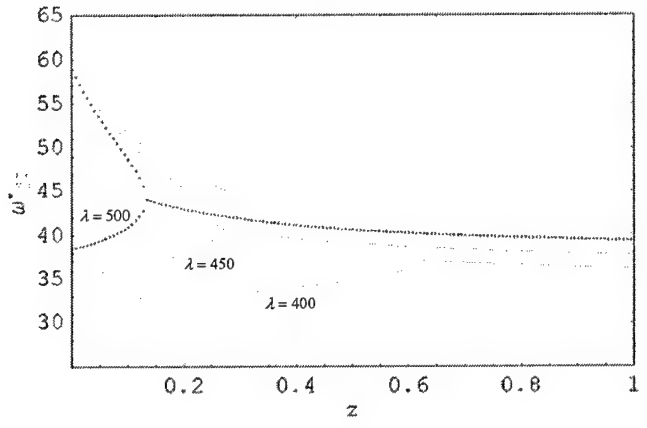

(b)

Figure 3. Dependence of real and imaginary parts of the panel natural frequency on relaxation parameter z for $\zeta = 0; \hat{\zeta} = 0.1; \bar{N}_0 = 0$ (a) real parts, (b) imaginary parts.

$\_\_\lambda = 400$; ..... $\lambda = 450$; ..... $\lambda = 500$

III. STABILITY AND LIMIT CYCLE OSCILLATIONS

The stability analysis is carried out by estimating the natural frequencies of the six modes in the absence of system nonlinearities and by setting the non-homogeneous term in equation (14) to zero. The dependence of the real and imaginary components of the eigenvalues on the dynamic pressure is shown in Figures 2(a) and (b) for three different values of relaxation parameter ($z = 0.001$, 0.1, and 1), damping parameter, $\zeta = 0.0$, mass parameter $\hat{\zeta} = 0.1$, and static axial load parameter $\bar{N}_0 = 0$. It is seen that the real parts are zero up to a critical value of the dynamic pressure, depending on the value of the relaxation parameter, z, above which one becomes negative and the other positive indicating the occurrence of panel instability. Note that the value $z = 0.0$ corresponds to a clamped-clamped panel, while $z = \infty$ corresponds to simple supports. The dependence of the components of the first and second eigenvalues on the relaxation parameter, z, is shown for three different values of dynamic pressure, $\lambda = 400$, 450, and 500, and the same parameters as Figure 2. It is seen that the eigenvalues possesses negative real parts up to a critical value of relaxation parameter, above which one eigenvalue has a positive real part indicating the occurrence of flutter.

Figures 4 and 5 show the boundaries of panel flutter in terms of the critical value of aerodynamic pressure, λ_{cr}, and the relaxation parameter, z. Figures 4 and 5 depict the influence of the in-plane load, $\bar{N}_0$, and damping ratio, ζ, respectively. As expected, the compression in-plane loading results in a reduction of the critical flutter speed. The clamped panel ($z << 1$) requires more in-plane compression load to reach its flutter speed. Figure 6 shows the dependence of flutter speed on the damping parameter, ζ. For a given relaxation parameter, there is a critical damping ratio, ζ_{cr}, above which the damping becomes beneficial and the critical speed increases with the damping. The value of ζ_{cr} is shown by a small circle on each curve and the locus of these points is shown by the dotted curve. For $\zeta < \zeta_{cr}$ the damping is detrimental and results in a reduction the

flutter speed. The critical damping ratio is determined by setting $d\lambda/d\zeta = 0$ and the dashed curve in Figure 6 shows the locus of the critical damping ratio.

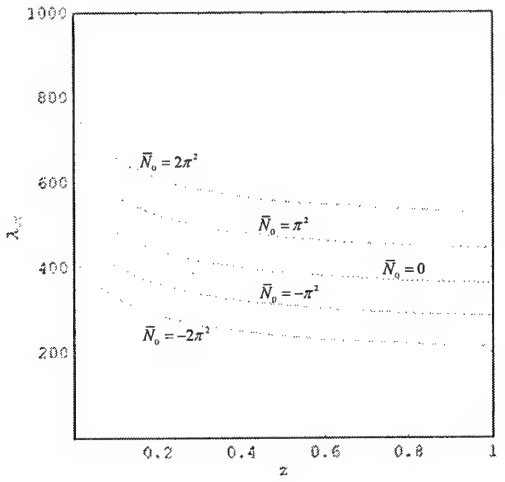

Figure 4. Boundaries of panel flutter on the plane for different values of in-plane load and for.

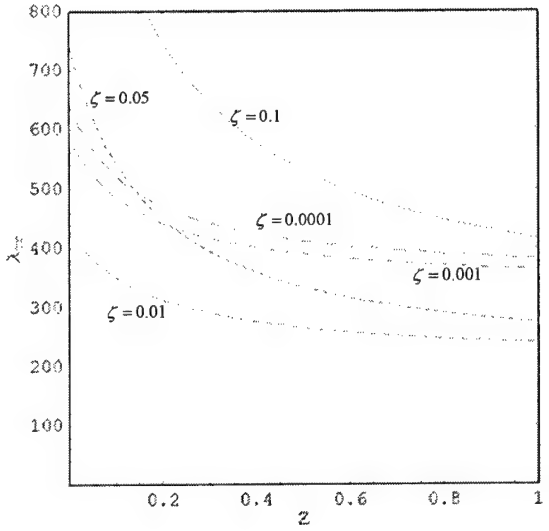

Figure 5. Boundaries of panel flutter on the plane for different values of damping factor showing the reversal effect of damping for ζ_{cr}.

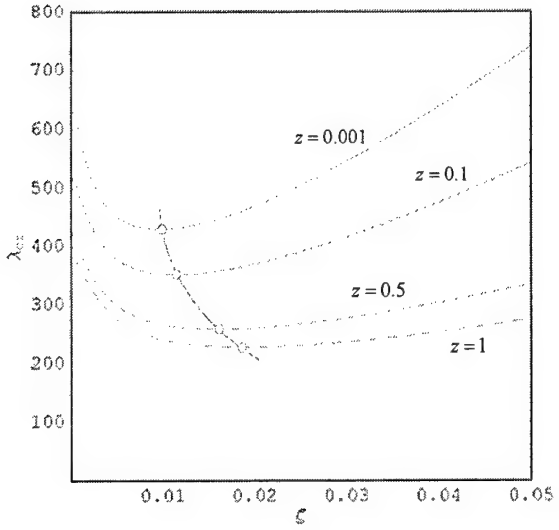

Figure 6. Boundaries of panel flutter on the $\lambda - \zeta$ plane for different values of relaxation parameter, z, and for $\overline{N}_0 = 0.0$; $\hat{\zeta} = 0.1$. Dashed curve indicates the critical damping ratio that separate between stabilizing and destabilizing damping effects.

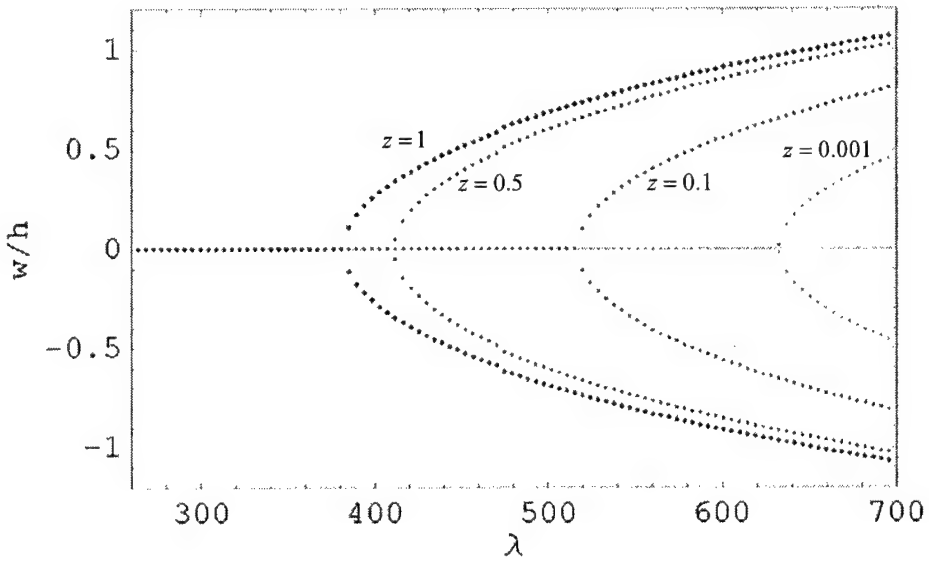

Figure 7. Bifurcation diagram for different values of relaxation parameter for $\zeta = 0.0001$, $\hat{\zeta} = 0.1$, $\overline{p}_0 = 0$, and $\overline{N}_0 = 0$.

Figures 7 show the dependence of limit cycle oscillation (LCO) amplitude on dynamic pressure for zero in-plane loading and different discrete values of the relaxation parameter z in the form of supercritical bifurcation. Note that relaxation results in moving the bifurcation point to lower values of dynamic pressure. Under compression in-plane loading, $\bar{N}_0 = -3\pi^2$ and under low values of dynamic pressure the panel experiences static buckling as shown in Figure 8. As the dynamic pressure increases the panel enters a stable state until the dynamic pressure reaches the critical value, λ_{cr}, above which the panel exhibits LCO. This scenario of buckled, straight, and LCO states is well known (see, e.g., Dowell, 1966) and is shown in the stability regions (see Figure 9) estimated for the case, $z = 1$. A three-dimensional diagram demonstrating the time evolution of LCO amplitude and their dependence on the dynamic pressure is shown in Figure 10 for zero in-plane loading and same parameters as in the previous figures. Note that the time over which relaxation takes place is demonstrated in Figure 11(a).

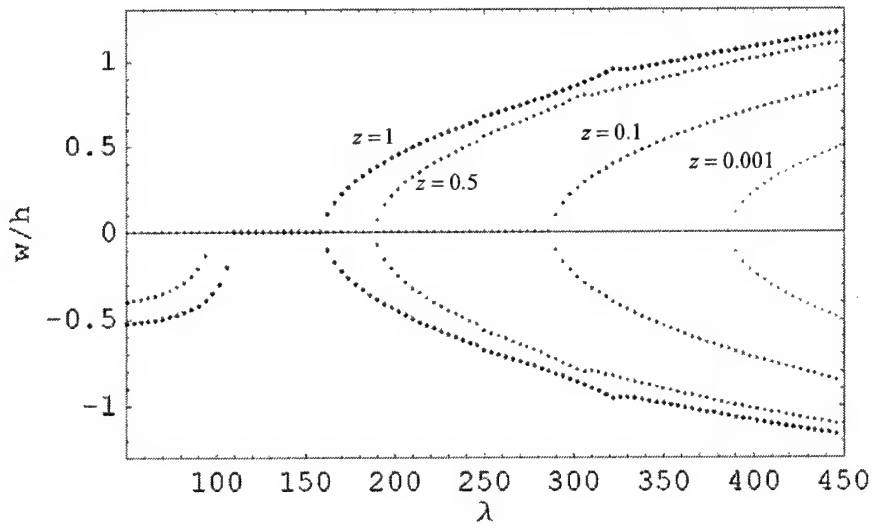

Figure 8. Bifurcation diagram for different values of relaxation parameter for $\zeta = 0.0001$, $\hat{\zeta} = 0.1$, $\bar{p}_0 = 0$, and $\bar{N}_0 = -3\pi^2$.

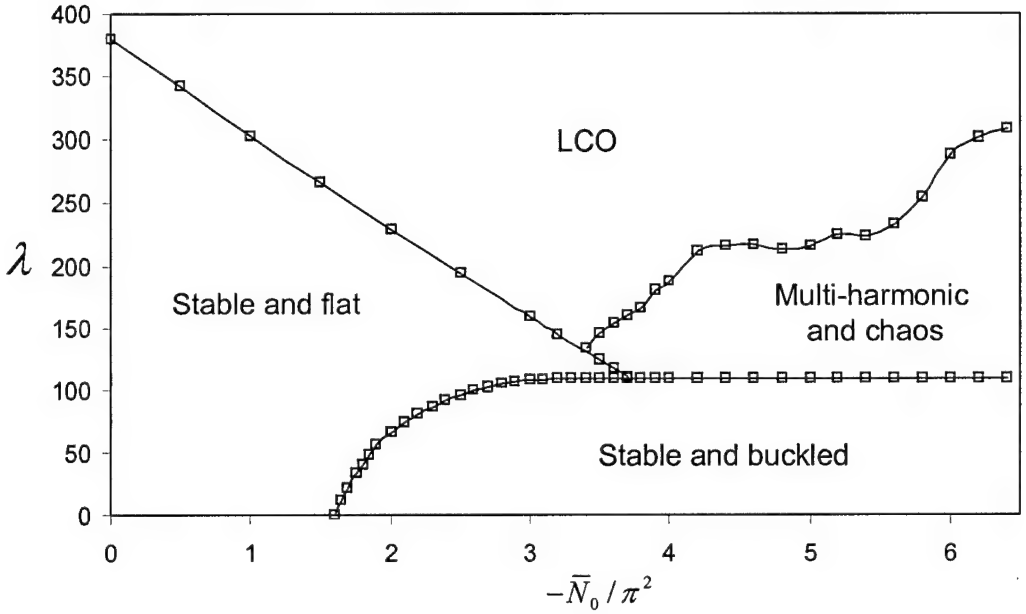

Figure 9.. Stability regions for $z=1$, $\zeta=0.0001, \hat{\zeta}=0.1$, $\bar{p}_0=0$

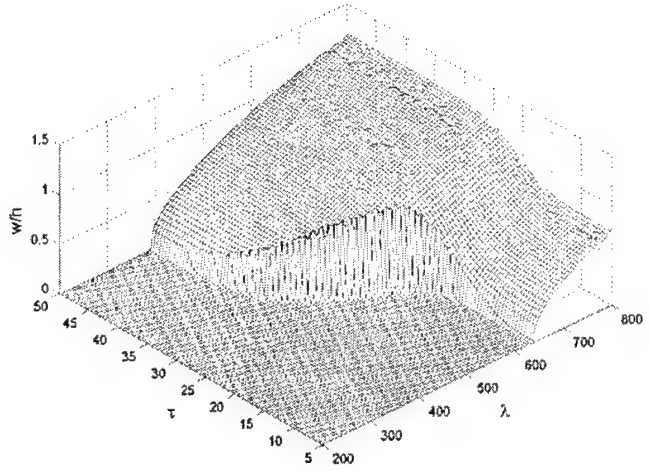

Figure 10. Three-dimensional plots of amplitudes time evolutions and their dependence on dynamic pressure for $\zeta=0.001$, $\hat{\zeta}=0.1$, $\bar{p}_0=1$, and $N_0=0$.

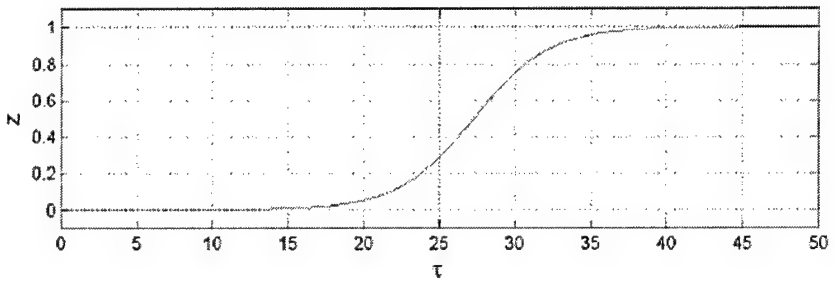

(a) Relaxation time history record

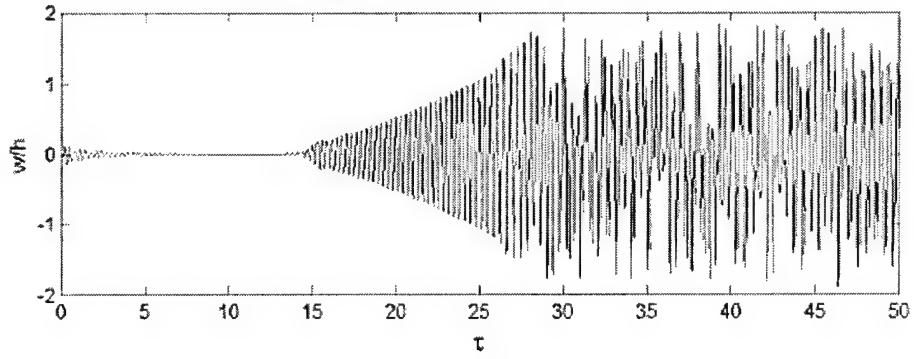

(b) Panel deflection time history for $\zeta = 0.0001$, $\bar{p}_0 = 0$, $\hat{\zeta} = 0.1$, $\bar{N}_0 = -6\pi^2$, and $\lambda = 200$

Figure 11. (a) Relaxation of boundary conditions and (b) time history record of panel deflection at $x/a = 0.75$

Under the relaxation curve shown in Figure 11(a), the time history record of the total deflection at $x/a = 0.75$ is shown in Figure 11(b) for in-plane compression loading, $\bar{N}_0 = -6\pi^2$, dynamic pressure, $\lambda = 200$. Over the whole time domain, the panel experiences two different regimes of oscillations, (1) growing amplitude limit cycle oscillations, and (2) chaotic oscillations. If the dynamic pressure is reduced, say $\lambda = 150$, the second regime exhibits snap-through irregular oscillations. For higher values of dynamic pressure, $\lambda \geq 500$, the time history records exhibit regular LCO with a center frequency that changes with time. Figures 12(a) and (b) show two cases of the FFT plots and spectrograms of the panel total deflection for the cases of (a) $\lambda = 700$, and $\zeta = 0.0001$, and (b) $\lambda = 700$, and $\zeta = 0.02$, respectively. It is seen that for low damping, Figure 12(a) the panel frequency decreases with time as the panel boundary conditions approach the case of simple supports. On the other hand, as the damping increases, the panel frequency increases with time. Note there are two factors competing with other,

namely, the structure's geometric nonlinearity and the relaxation in the boundary conditions. By increasing the damping factor, the structure geometric nonlinearity overcomes the influence of relaxation and the frequency increases as shown in Figure 12(b).

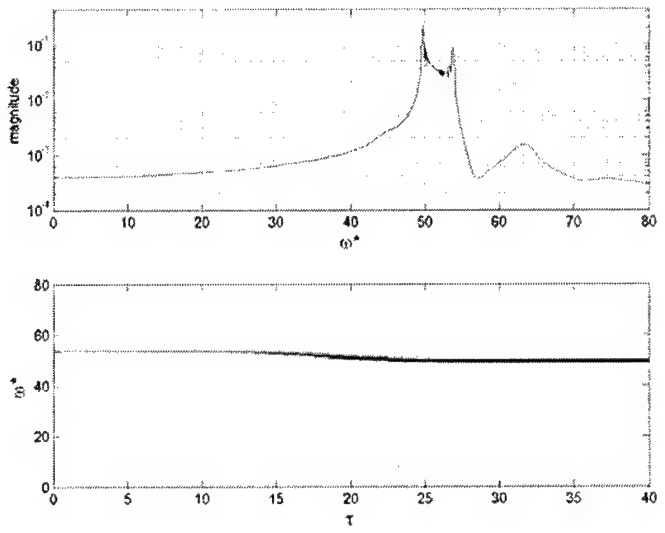

(a)

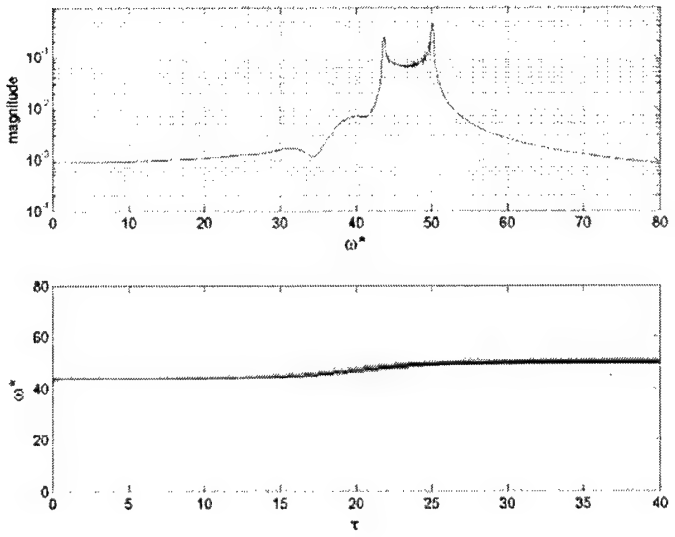

(b)

Figure 12 FFT plots and spectrograms for $\overline{p}_0 = 0,\ \overline{N}_0 = 0,\ \hat{\zeta} = 0.1$
(a) $\lambda = 700, \zeta = 0.0001$, (b) $\lambda = 700, \zeta = 0.02$.

The bifurcation diagram shown in Figure 13 reveals different regimes of panel dynamic behavior. The figure is obtained by plotting the first return points of the panel amplitude as the dynamic pressure varies for relation parameter, $z=1$, and in-plane loading $\bar{N}_0=-5\pi^2$. The bifurcation begins with the buckled state up to $\lambda=109$, chaotic motion over the region $109<\lambda<140$, period 3 over the region $140<\lambda<160$, then a region of chaotic motion mixed strips of period n occupying the range $160<\lambda<215$, Above $\lambda>215$ the panel possesses regular limit cycle oscillations. Figure 14 shows another bifurcation diagram where the relaxation parameter, z, is taken as the control parameter, for dynamic pressure $\lambda=250$, and in-plane pressure, $\bar{N}_0=-5.8\pi^2$. For $0<z<0.43$, the panel experiences LCO with varying amplitude. This region is followed by a cascade of multi-periods up to $z\approx 0.81$, above which the panel exhibits chaotic oscillations. Time history records corresponding to z=0.4, 0.7735, and 1, are shown in Figure 15. The corresponding phase diagrams and FFT plots of these time history records are shown in Figure 16.

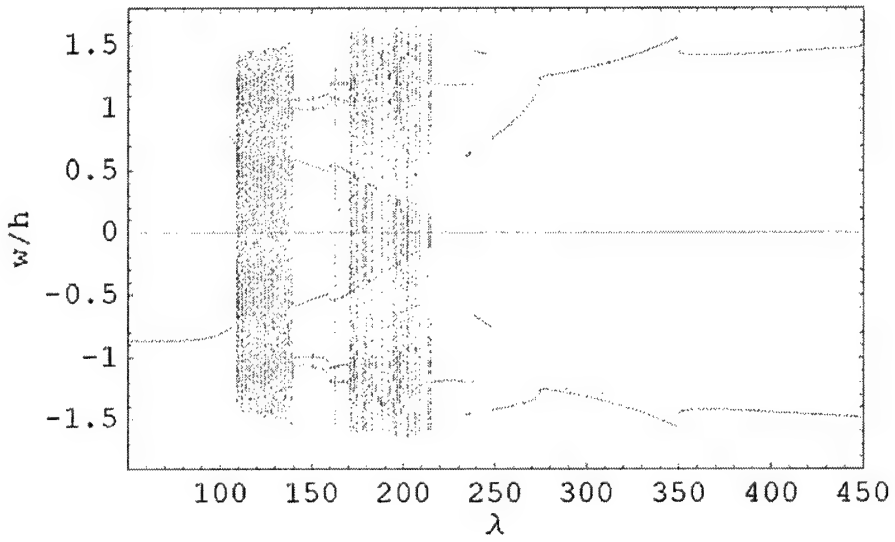

Figure 13. Bifurcation diagram for $\zeta=0.0001$, $\bar{p}_0=0$, $\hat{\zeta}=0.1$, $\bar{N}_0=-5\pi^2$, and $z=1$

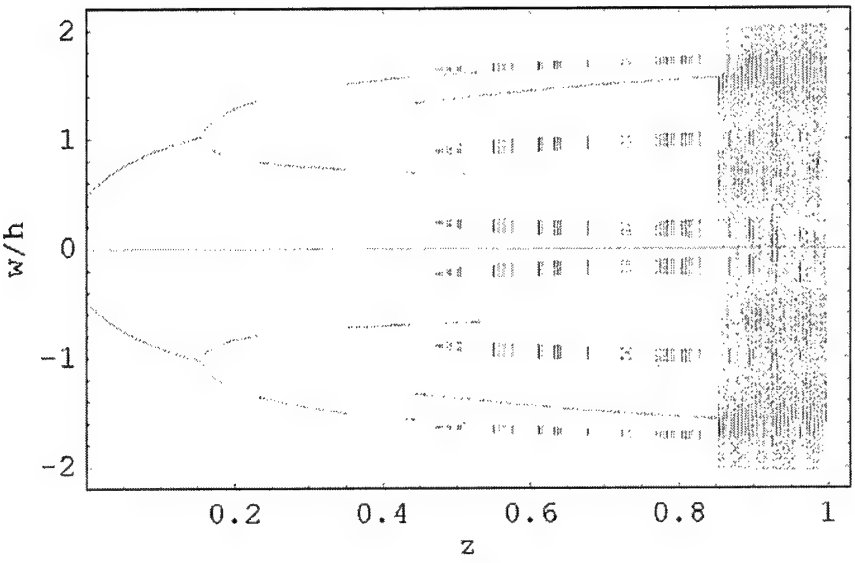

Figure 14. Bifurcation diagram for $\zeta = 0.0001$, $\overline{p}_0 = 0$, $\hat{\zeta} = 0.1$, $\overline{N}_0 = -5.8\pi^2$, and $\lambda = 250$

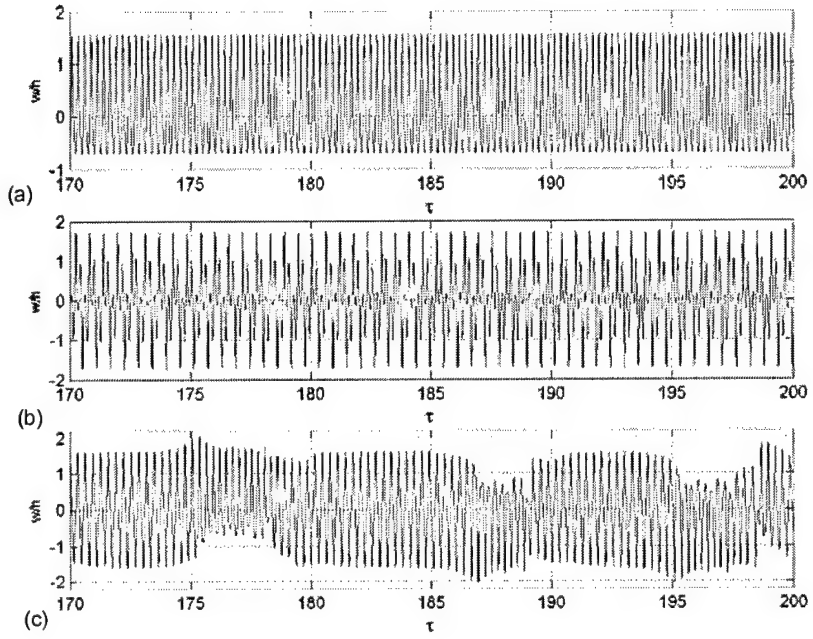

Figure 15. Time history sections for $\zeta = 0.0001$, $\overline{p}_0 = 0$, $\hat{\zeta} = 0.1$, $\overline{N}_0 = -5.8\pi^2$, and $\lambda = 250$: (a) $z = 0.4$; (b) $z = 0.7735$; (c) $z = 1$

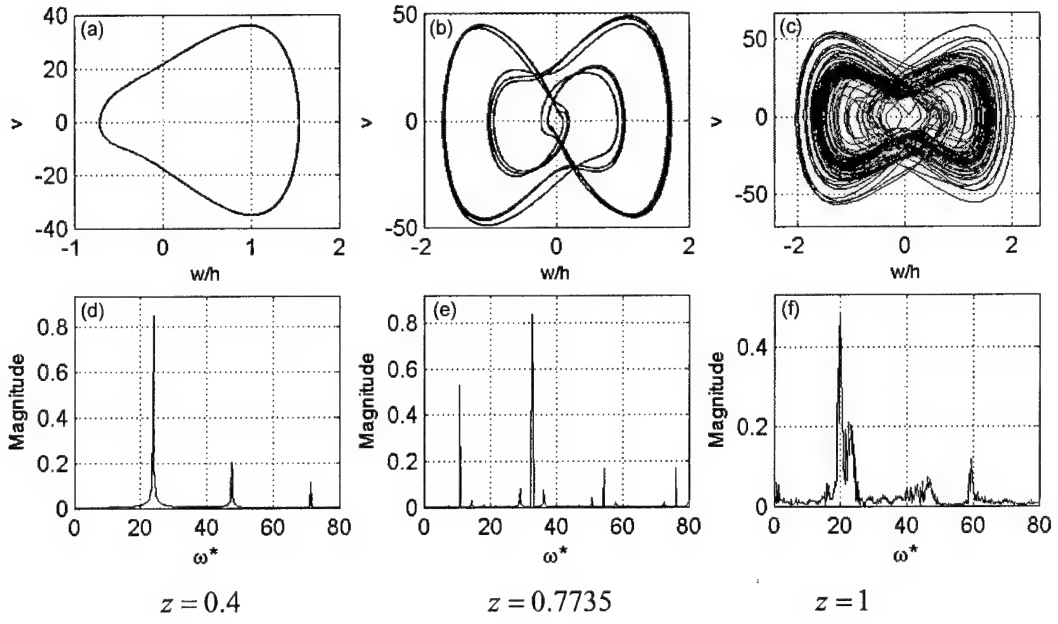

Figure 16. Phase plots and FFT of time history records of Figure 15.

IV. CONCLUSIONS

The nonlinear flutter of a two-dimensional panel exposed to supersonic gas flow involving six-mode interaction is studied in the presence of non-ideal boundary conditions. The deterministic study includes stability analysis in terms of dynamic pressure, relaxation parameter, damping ratio, and in-plane loading. For in-plane loading below the critical buckling value, the panel experiences LCO above a critical aerodynamic pressure governed by the relaxation parameter. For compressive in-plane loads, the panel experiences periodic, quasi-periodic and chaotic oscillations depending on the values of dynamic pressure, relaxation parameter and damping ratios.

APPENDIX

$$M(\tau)=\begin{bmatrix} 1 & 0 & m_{13} & 0 & m_{15} & 0 \\ 0 & 1 & 0 & m_{24} & 0 & m_{26} \\ m_{31} & 0 & 1 & 0 & m_{35} & 0 \\ 0 & m_{42} & 0 & 1 & 0 & m_{46} \\ m_{51} & 0 & m_{53} & 0 & 1 & 0 \\ 0 & m_{52} & 0 & m_{64} & 0 & 1 \end{bmatrix}, \qquad m_{13}(\tau)=-\frac{9}{4[3+\pi^2(1+6z(\tau))]}$$

$$C=\begin{bmatrix} \zeta b_{11}+\hat{\zeta}\sqrt{\lambda} & 0 & \zeta b_{12}+\hat{\zeta}b_{13}\sqrt{\lambda} & 0 & \zeta b_{14}+\hat{\zeta}b_{15}\sqrt{\lambda} & 0 \\ 0 & \zeta b_{21}+\hat{\zeta}\sqrt{\lambda} & 0 & \zeta b_{22}+\hat{\zeta}b_{23}\sqrt{\lambda} & 0 & \zeta b_{24}+\hat{\zeta}b_{25}\sqrt{\lambda} \\ \zeta b_{31}+\hat{\zeta}b_{32}\sqrt{\lambda} & 0 & \zeta b_{33}+\hat{\zeta}\sqrt{\lambda} & 0 & \zeta b_{34}+\hat{\zeta}b_{35}\sqrt{\lambda} & 0 \\ 0 & \zeta b_{41}+\hat{\zeta}b_{42}\sqrt{\lambda} & 0 & \zeta b_{43}+\hat{\zeta}\sqrt{\lambda} & 0 & \zeta b_{44}+\hat{\zeta}b_{45}\sqrt{\lambda} \\ \zeta b_{51}+\hat{\zeta}b_{52}\sqrt{\lambda} & 0 & \zeta b_{53}+\hat{\zeta}b_{54}\sqrt{\lambda} & 0 & \zeta b_{55}+\hat{\zeta}\sqrt{\lambda} & 0 \\ 0 & \zeta b_{61}+\hat{\zeta}b_{62}\sqrt{\lambda} & 0 & \zeta b_{63}+\hat{\zeta}b_{64}\sqrt{\lambda} & 0 & \zeta b_{65}+\hat{\zeta}\sqrt{\lambda} \end{bmatrix}$$

$$b_{11}(\tau)=\frac{\pi^4[51+\pi^2(1+6z(\tau))]}{3+\pi^2(1+6z(\tau))}.$$

$$K=\begin{bmatrix} c_{11}\bar{N}_0+c_{12} & c_{13}\lambda+c_{14} & c_{15}\bar{N}_0+c_{16} & c_{17}\lambda+c_{18} & c_{19}\bar{N}_0+c_{110} & c_{111}\lambda+c_{112} \\ c_{21}\lambda+c_{22} & c_{23}\bar{N}_0+c_{24} & c_{25}\lambda+c_{26} & c_{27}\bar{N}_0+c_{28} & c_{29}\lambda+c_{210} & c_{211}\bar{N}_0+c_{212} \\ c_{31}\bar{N}_0+c_{32} & c_{33}\lambda+c_{34} & c_{35}\bar{N}_0+c_{36} & c_{37}\lambda+c_{38} & c_{39}\bar{N}_0+c_{310} & c_{311}\lambda+c_{312} \\ c_{41}\lambda+c_{42} & c_{43}\bar{N}_0+c_{44} & c_{45}\lambda+c_{46} & c_{47}\bar{N}_0+c_{48} & c_{49}\lambda+c_{410} & c_{411}\bar{N}_0+c_{412} \\ c_{51}\bar{N}_0+c_{52} & c_{53}\lambda+c_{54} & c_{55}\bar{N}_0+c_{56} & c_{57}\lambda+c_{58} & c_{59}\bar{N}_0+c_{510} & c_{511}\lambda+c_{512} \\ c_{61}\lambda+c_{62} & c_{63}\bar{N}_0+c_{64} & c_{65}\lambda+c_{66} & c_{67}\bar{N}_0+c_{68} & c_{69}\lambda+c_{610} & c_{611}\bar{N}_0+c_{612} \end{bmatrix}$$

$$D=\begin{bmatrix} d_{11} & 0 & d_{13} & 0 & d_{15} & 0 \\ 0 & d_{22} & 0 & d_{24} & 0 & d_{26} \\ d_{31} & 0 & d_{33} & 0 & d_{35} & 0 \\ 0 & d_{42} & 0 & d_{44} & 0 & d_{46} \\ d_{51} & 0 & d_{53} & 0 & d_{55} & 0 \\ 0 & d_{62} & 0 & d_{64} & 0 & d_{66} \end{bmatrix},$$

$$d_{11}(\tau)=\frac{1}{60}[-15+10\pi^2(1+3z(\tau)+\pi^4(1+10z(\tau)+30z^2(\tau))]B_1$$

$$\left\{eq_i q_j^2\right\}=\begin{Bmatrix} e_{11}q_1q_2^2+e_{12}q_1q_3^2+e_{13}q_1q_4^2+e_{14}q_1q_5^2+e_{15}q_1q_6^2+e_{16}q_3q_1^2+e_{17}q_3q_2^2+e_{18}q_3q_4^2+ \\ e_{21}q_2q_1^2+e_{22}q_2q_3^2+e_{23}q_2q_4^2+e_{24}q_2q_5^2+e_{25}q_2q_6^2+e_{26}q_4q_1^2+e_{27}q_4q_2^2+e_{28}q_4q_3^2+ \\ e_{31}q_1q_2^2+e_{32}q_1q_3^2+e_{33}q_1q_4^2+e_{34}q_1q_5^2+e_{35}q_1q_6^2+e_{36}q_3q_1^2+e_{37}q_3q_2^2+e_{38}q_3q_4^2+ \\ e_{41}q_2q_1^2+e_{42}q_2q_3^2+e_{43}q_2q_4^2+e_{44}q_2q_5^2+e_{45}q_2q_6^2+e_{46}q_4q_1^2+e_{47}q_4q_2^2+e_{48}q_4q_3^2+ \\ e_{51}q_1q_2^2+e_{52}q_1q_3^2+e_{53}q_1q_4^2+e_{54}q_1q_5^2+e_{55}q_1q_6^2+e_{56}q_3q_1^2+e_{57}q_3q_2^2+e_{58}q_3q_4^2+ \\ e_{61}q_2q_1^2+e_{62}q_2q_3^2+e_{63}q_2q_4^2+e_{64}q_2q_5^2+e_{65}q_2q_6^2+e_{66}q_4q_1^2+e_{67}q_4q_2^2+e_{68}q_4q_3^2+ \end{Bmatrix}$$

$$\begin{Bmatrix} +e_{19}q_3q_5^2+e_{110}q_3q_6^2+e_{111}q_5q_1^2+e_{112}q_5q_2^2+e_{113}q_5q_3^2+e_{114}q_5q_4^2+e_{115}q_5q_6^2 \\ +e_{29}q_4q_5^2+e_{210}q_4q_6^2+e_{211}q_6q_1^2+e_{212}q_6q_2^2+e_{213}q_6q_3^2+e_{214}q_6q_4^2+e_{215}q_6q_5^2 \\ +e_{39}q_3q_5^2+e_{310}q_3q_6^2+e_{311}q_5q_1^2+e_{312}q_5q_2^2+e_{313}q_5q_3^2+e_{314}q_5q_4^2+e_{315}q_5q_6^2 \\ +e_{49}q_4q_5^2+e_{410}q_4q_6^2+e_{411}q_6q_1^2+e_{412}q_6q_2^2+e_{413}q_6q_3^2+e_{414}q_6q_4^2+e_{415}q_6q_5^2 \\ +e_{59}q_3q_5^2+e_{510}q_3q_6^2+e_{511}q_5q_1^2+e_{512}q_5q_2^2+e_{513}q_5q_3^2+e_{514}q_5q_4^2+e_{515}q_5q_6^2 \\ +e_{69}q_4q_5^2+e_{610}q_4q_6^2+e_{611}q_6q_1^2+e_{612}q_6q_2^2+e_{613}q_6q_3^2+e_{614}q_6q_4^2+e_{615}q_6q_5^2 \end{Bmatrix},$$

$$e_{11}(\tau)=\frac{1}{240}[-15+40\pi^2(1+3z(\tau))+16\pi^4(1+10z(\tau)+30z^2(\tau))]B_1$$

$$\left\{fq_iq_jq_k\right\}=\begin{Bmatrix} f_{11}q_1q_2q_4+f_{12}q_1q_2q_6+f_{13}q_1q_3q_5+f_{14}q_1q_4q_6+f_{15}q_2q_3q_4+ \\ f_{21}q_1q_2q_3+f_{22}q_1q_3q_4+f_{23}q_1q_2q_5+f_{24}q_2q_3q_5+f_{25}q_1q_4q_5+ \\ f_{31}q_1q_2q_4+f_{32}q_1q_2q_6+f_{33}q_1q_3q_5+f_{34}q_1q_4q_6+f_{35}q_2q_3q_4+ \\ f_{41}q_1q_2q_3+f_{42}q_1q_3q_4+f_{43}q_1q_2q_5+f_{44}q_2q_3q_5+f_{45}q_1q_4q_5+ \\ f_{51}q_1q_2q_4+f_{52}q_1q_2q_6+f_{53}q_1q_3q_5+f_{54}q_1q_4q_6+f_{55}q_2q_3q_4+ \\ f_{61}q_1q_2q_3+f_{62}q_1q_3q_4+f_{63}q_1q_2q_5+f_{64}q_2q_3q_5+f_{65}q_1q_4q_5+ \end{Bmatrix}$$

$$\begin{Bmatrix} +f_{16}q_2q_3q_6+f_{17}q_2q_4q_5+f_{18}q_2q_5q_6+f_{19}q_3q_4q_6+f_{110}q_4q_5q_6 \\ +f_{26}q_2q_4q_6+f_{27}q_3q_4q_5+f_{28}q_1q_3q_6+f_{29}q_3q_5q_6+f_{210}q_1q_5q_6 \\ +f_{36}q_2q_3q_6+f_{37}q_2q_4q_5+f_{38}q_2q_5q_6+f_{39}q_3q_4q_6+f_{310}q_4q_5q_6 \\ +f_{46}q_2q_4q_6+f_{47}q_3q_4q_5+f_{48}q_1q_3q_6+f_{49}q_3q_5q_6+f_{410}q_1q_5q_6 \\ +f_{56}q_2q_3q_6+f_{57}q_2q_4q_5+f_{58}q_2q_5q_6+f_{59}q_3q_4q_6+f_{510}q_4q_5q_6 \\ +f_{66}q_2q_4q_6+f_{67}q_3q_4q_5+f_{68}q_1q_3q_6+f_{69}q_3q_5q_6+f_{610}q_1q_5q_6 \end{Bmatrix}, \quad f_{11}(\tau)=-\frac{16}{27}(22+15\pi^2z(\tau))B_1$$

$$\left\{P(\tau)\right\}=\begin{Bmatrix} 2\overline{p}_0/\pi \\ 0 \\ 3\overline{p}_0/2\pi \\ 0 \\ 5\overline{p}_0/3\pi \\ 0 \end{Bmatrix}$$

References

Ashly, H., and Zartarian, G., 1956, "Piston Theory – A New Aerodynamic Tool for Aeroelastician," *Journal of the Aeronautical Science* **23**(10), 1109-1118.

Bickford, J. H., 1990, *An Introduction to the Design and Behavior of Bolted Joints*, 2nd edition, Marcel Dekker, Inc., New York.

Bolotin, V.V., Grishko, A.A., Kounadis, A.N., and Gantes, C.J., 1998, Non-Linear Panel Flutter in Remote Postcritical Domains, *International Journal of Non-Linear Mechanics* **33**(5), 753-764.

Bolotin, V.V., Grishko, A.A., and Panov, M.Yu., 2002, Effect of Damping on the Postcritical Behavior of Autonomous Non-Conservative System, *International Journal of Non-Linear Mechanics* **37**, 1163-1179.

Dowell, E. H., 1982, "Flutter of a Buckled Plate as an Example of Chaotic motion of a Deterministic Autonomous System," *Journal of Sound and Vibration* **85**(3), 333-344.

Dowell, E. H., 1984, "Observation and Evolution of Chaos for an Autonomous System," *ASME Journal of Applied Mechanics* **51**(1), 664-673.

Epureanu, B.I., Liaosha, S.T., Paidoussis, M.P., 2004, Coherent Structures and their Influence on the Dynamics of Aeroelastic Panels, *International Journal of Non-Linear Mechanics* **39**, 977-991

Ibrahim, R. A., 1987, "Structural Dynamics with Parameter Uncertainties," *ASME Appl Mech Rev* **40**(3), 309-328.

Ibrahim, R. A., Orono, P. O. and Madaboosi, S. R., 1990, "Stochastic Flutter of a Panel Subjected to Random In-Plane Forces, Part I: Two Mode Interaction," *AIAA Journal*, **28**(4), pp. 694-702.

Ibrahim, R. A., and Pettit, C. L. (2004), "Uncertainties and Dynamic Problems of Bolted Joints and Other Fasteners," *Journal of Sound and Vibration*, in press.

Ibrahim, R. A., Beloiu, D. M. and Pettit, C. L., 2004, "Influence of Joint Relaxation on Reterministic and Stochastic Panel Flutter," *AIAA Journal*, in press.

Kuo, C.C., Morino, L., and Dugundji, J., 1972, Perturbation and Harmonic Balance Methods for nonlinear panel flutter, *AIAA Journal* **10**, p. 1479

Lindsley, N. J., Beran, P. S., and Pettit, C. L., 2002a, "Effects of uncertainty on nonlinear plate response in supersonic flow," 9th AIAA Symp *Multidisciplinary Analysis and Optimization*, Atlanta, GA, Paper 2002-5600.

Lindsley, N. J., Beran, P. S., and Pettit, C. L., 2002b, "Effects of uncertainty on nonlinear plate aeroelastic response," 43rd AIAA/ASME/ASCE/AHS/ASCE *Struct Struct Dyn Mater* Conf. Paper No. AIAA 2002-1271.

Manohar, C. S. and Ibrahim, R. A., 1999, Progress in Structural Dynamics with Stochastic Parameter Variations: 1987-1998," *ASME Appl. Mech Rev* **52**(5), 177-197.

Poiron, B., 1995, "Impact of Random Uncertainties on Aircraft Aeroelastic Stability," Proc. Stochastic Structural Dynamics Conference, San Juan, Puerto Rico.

Pourtakdoust, S.H., and Fazelzadeh, S.A., 2003, Chaotic Analysis of Nonlinear Viscoelastic Panel Flutter in Supersonic Flow, *Nonlinear Dynamics* **32**, 387-404.

Qiao, S., Pilipchuk, V. N. and Ibrahim, R. A., 2000, "Modeling and simulation of elastic structures with parameter uncertainties and relaxation of joints," *ASME J Vib Acoust* **123**(1), 45-52.

INFLUENCE OF JOINT RELAXATION ON DETERMINISTIC AND STOCHASTIC PANEL FLUTTER

R.A. Ibrahim, D.M. Beloiu
Wayne State University, Department of Mechanical Engineering, Detroit MI 48202, USA
C.L. Pettit
Air Force Research Laboratory, AFRL/VASD, Wright-Patterson Air Force Base, OH 45433, USA

ABSTRACT

The influence of boundary conditions relaxation on two-dimensional panel flutter is studied in the absence and presence of random in-plane loading. The boundary value problem of the panel involves time-dependent boundary conditions that are converted into autonomous form using a special coordinate transformation. The analysis is restricted to two-mode interaction and includes the influence of boundary conditions relaxation on the panel modal frequencies and limit cycle amplitudes in the time and frequency domains using spectrogram technique. The relaxation and system nonlinearity are found to have opposite effects on the frequency evolution of the panel. Furthermore, the damping of the panel exhibits a critical value governed by the relaxation parameter, below which the damping has a destabilizing effect and above that critical value it has stabilizing effect. Stochastic stability boundaries under random in-plane loading are estimated below the critical aerodynamic pressure. Depending on the system damping and dynamic pressure, the evolution of the panel frequency content can increase or decrease with time as the panel approaches near simply supported boundary conditions.

1. INTRODUCTION

Panel flutter under deterministic and stochastic airflow has been extensively studied based on simplified modeling of the structure, aerodynamics, and boundary conditions. Most of the analyses of panel flutter are based on ideal boundary conditions such as clamped or simple supported edges. However, most fasteners do not satisfy absolute boundary conditions. In addition, fasteners subjected to vibration often lose much of their preload; this is known as relaxation. Vibration-induced loosening and relaxation effects cause time-dependent boundary conditions and depend on the level of structural vibration. Recently, Ibrahim and Pettit (2004) presented an extensive review of dynamic problems associated with joint relaxation and uncertainties.

A limited number of studies have considered the influence of uncertainties in aeroelastic structures and their boundary conditions. For example, Poiron (1995) introduced uncertainties in analyzing the flutter characteristics of aircraft models. The effect of uncertainty in the boundary conditions, combined with the variability of material properties, on nonlinear panel aeroelastic response was studied by Lindsley et al (2002a,b). Although Lindsley et al (2002a,b) considered the effect of variability in boundary rotational stiffness, none of the studies cited above included the influence of time-dependent boundary conditions on the flutter characteristics of aeroelastic structures. Relaxation, or the loss of pre-load in mechanical joints, is a common problem in vibrating structures that must be addressed to ensure that the structure will perform satisfactorily throughout its expected life. The present work is an extension of the work of Ibrahim et al (1990, 1991, 2003) and Qiao et al (2000) to examine the influence of relaxation of boundary conditions on the panel flutter characteristics such as modal natural frequencies and limit cycle amplitudes, and stochastic stability under random in-plane loading.

Nonlinear panel flutter with relaxation in the boundary conditions is studied based on a phenomenological model of joint preload relaxation and random aerodynamic pressure superposed on piston theory. The conventional boundary value problem of the panel involves time-dependent boundary conditions that are converted to an autonomous form using a special coordinate transformation introduced by Qiao et al (2000). The resulting boundary conditions are combined with the governing non-homogeneous, partial differential equation that includes the influence of the boundary condition relaxation. The analysis is restricted to two-mode interaction. Results include the influence of boundary condition relaxation on the panel stability boundaries, modal frequencies, limit cycle amplitudes in the time and frequency domains, and mean square stability.

2. ANALYSIS

The governing equation of motion of a two-dimensional panel under supersonic flow is developed using Hamilton's principle. In order to estimate the work done by aerodynamic loading, the pressure on the panel is estimated using piston theory with quadratic nonlinearity. With reference to Figure 1, the governing nonlinear equation of motion for the panel is

$$m_p\frac{\partial^2 w}{\partial t^2}+D\left(1+c\frac{\partial}{\partial t}\right)\frac{\partial^4 w}{\partial x^4}-\left[N_{x0}(t)+\frac{Eh}{2a}\int_0^a\left(\frac{\partial w}{\partial x}\right)^2 dx\right]\frac{\partial^2 w}{\partial x^2}+\frac{\rho_\infty U_\infty^2}{M}\left[\frac{\partial w}{\partial x}+\frac{1}{U_\infty}\frac{\partial w}{\partial t}\right]+\rho_\infty\frac{(\gamma+1)}{4}\left[\left(\frac{\partial w}{\partial t}\right)^2+2U_\infty\frac{\partial w}{\partial t}\frac{\partial w}{\partial x}+U_\infty^2\left(\frac{\partial w}{\partial x}\right)^2\right]=\Delta p_0 \tag{1}$$

where $w(x,t)$ is the panel deflection, m_p is the panel mass per unit area, a is the panel length, E is Young's modulus, h is the plate thickness, $D=Eh^3/(12(1-\nu^2))$, and ν is Poisson's ratio.

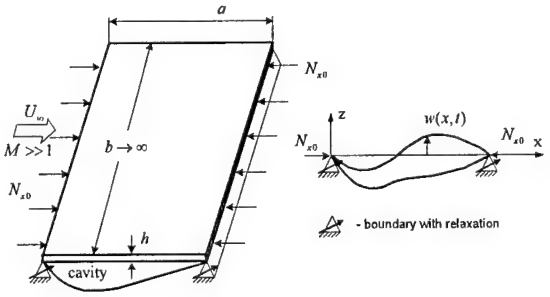

Figure 1 Schematic diagram of a two-dimensional panel exposed to supersonic flow

Δp_0 is the air pressure difference through the panel, $N_{x0}(t)=N_{x0}+N_x(t)$ is the external in-plane load per unit span-wise length and may be random in time, and c is a linear viscous damping coefficient. Equation (1) is subject to the boundary conditions

$$D\frac{\partial^2 w(0,t)}{\partial x^2}-\alpha_1(t)\frac{\partial w(0,t)}{\partial x}=0,\quad w(0,t)=0 \tag{2a,b}$$

$$D\frac{\partial^2 w(a,t)}{\partial x^2}+\alpha_2(t)\frac{\partial w(a,t)}{\partial x}=0,\quad w(a,t)=0 \tag{2c,d}$$

where $\alpha_1(t)$ and $\alpha_2(t)$ represent torsional stiffness parameters such that for $\alpha_1(t)=\alpha_1(t)=\infty$ we have the case of purely clamped-clamped panel. For simple supports, we have $\alpha_1(t)=\alpha_1(t)=0$. In real situations, both $\alpha_1(t)$ and $\alpha_2(t)$ do not assume these extreme cases and their values are very large for clamped supports, or very small for simple supports. In the dynamic case the boundary conditions (2a,c) are non-autonomous. In order to convert these conditions into an autonomous form, we introduce the following transformation of the response coordinate

$$w(x,t)=\varphi(x;z_1,z_2)u(x,t) \tag{3}$$

where $\varphi(x;z_1,z_2)$ is a transformation function and $u(x,t)$ is the new coordinate which satisfies the autonomous boundary conditions

$$\frac{\partial^2 u(0,t)}{\partial x^2}=\frac{\partial^2 u(a,t)}{\partial x^2}=0 \text{ and } u(0,t)=u(a,t)=0. \tag{4}$$

The transformation function $\varphi(x;z_1,z_2)$ depends on the dimensionless relaxation parameter $z_i(t)=D/a\alpha_i(t)$, $i=1,2$ representing the ratio of the bending rigidity to the torsional stiffness of the joints.

The governing equation of motion is discretized using Galerkin's method by assuming the expansion

$$\overline{u}(\overline{x},\tau)=\sum_{n=1}^{N}q_n(\tau)\sin n\pi\overline{x} \tag{5}$$

where N is the total number of modes, and $q_n(\tau)$ are the generalized coordinates. For the present study, we consider two-mode interaction. The following two nonlinear ordinary differential equations are obtained

$$q_1''(\tau)+(\zeta a_{11}+\hat{\zeta}\sqrt{\lambda})q_1'(\tau)+(a_{12}\overline{N}_{x0}(\tau)+a_{13})q_1(\tau)+(a_{14}\lambda+a_{15})q_2(\tau)+B_2b_{11}q_1'(\tau)^2+B_2b_{12}q_2'(\tau)^2+B_3b_{13}q_1'(\tau)q_2(\tau)+B_3b_{14}q_1(\tau)q_2'(\tau)+B_1b_{15}q_1(\tau)^3+B_1b_{16}q_1(\tau)q_2(\tau)^2+B_4b_{17}q_1(\tau)^2+B_4b_{18}q_2(\tau)^2=\frac{2\Delta\overline{p}_0(\tau)}{\pi}\frac{1}{c_0(\tau)} \tag{6a}$$

$$q_2''(\tau)+(\zeta a_{21}+\hat{\zeta}\sqrt{\lambda})q_2'(\tau)+(a_{22}\overline{N}_{x0}(\tau)+a_{23})q_2(\tau)+(a_{24}\lambda+a_{25})q_1(\tau)+B_2b_{21}q_1'(\tau)q_2'(\tau)+B_3b_{22}q_1'(\tau)q_1(\tau)+B_3b_{23}q_2(\tau)q_2'(\tau)+B_4b_{42}q_1(\tau)q_2(\tau)+B_1b_{25}q_2(\tau)^3+B_1b_{26}q_1(\tau)^2q_2(\tau)=0 \tag{6b}$$

where a prime denotes differentiation with respect

to the non-dimensional time parameter τ, the coefficients a_{ij} and b_{ij} are functions of the relaxation parameter $z(\tau)$, which is time dependent, and was derived by Ibrahim et al (2003)

$$z(\tau) = Z_0 Z_\infty \left[Z_0 - (Z_0 - Z_\infty) \frac{1 + \tanh(-\chi(\tau - \tau_c))}{1 + \tanh(\chi \tau_c)} \right]^{-1} \tag{7}$$

2.1 Deterministic Analysis

The deterministic analysis is carried out based on constant values of in-plane force $\bar{N}_{x0}(\tau) = \bar{N}_{x0}$. The influence of boundary conditions relaxation on the panel eigenvalues can be examined by dropping the nonlinear and non-homogeneous terms from the modal equations (6). The dependence of the real part on the dynamic pressure for different values of relaxation parameter is shown in Figure 2 where the crossing to positive values signals the occurrence of flutter. As expected, as the panel nears clamped boundary conditions the occurrence of flutter requires relatively higher values of dynamic pressure. The dependence of the critical value of aerodynamic pressure on the in-plane static load, $\bar{N}_{x0}$, damping ratio, ζ, and relaxation parameter, z, is shown in Figures 3, 4, and 5, respectively. These figures represent the boundaries of panel flutter for different values of the relaxation parameter as shown in Figures 3 and 4.

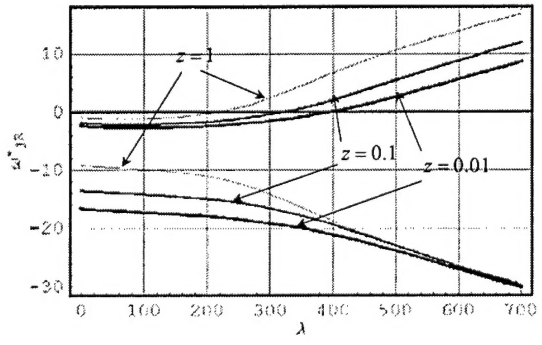

Figure 2 Dependence of real part of natural frequencies on the relaxation parameter for different values of dynamic pressure parameter λ *and for* $\zeta = 0.01$, $\hat{\zeta} = 0.1$, $N_0 = 0$.

As expected the compressive in-plane loading results in a reduction of the critical flutter speed. The clamped panel ($z << 1$) requires more in-plane compression load to reach its flutter speed. Figure 4 shows the dependence of flutter speed on the damping parameter ζ. For a given relaxation parameter, there is a critical damping ratio ζ_{cr} above which the damping becomes beneficial and the critical speed increases with the damping. For $\zeta < \zeta_{cr}$ the damping is non-beneficial and results in a reduction the flutter speed. The critical damping ratio is determined by setting $d\lambda_{cr} / d\zeta = 0$ and the dashed curve in Figure 4 shows the locus of the critical damping ratio. For equal modal viscous damping coefficients, the damping is known to stabilize the panel. However, as shown in Ibrahim, et al. (2003), and the references cited therein, unequal modal damping coefficients result in a paradoxical effect. Figure 5 shows the dependence of the flutter speed on the relaxation parameter for different values of static in-plane loading. The destabilizing effect of damping is shown in Figure 6, where the instability region increases as the damping increases then decreases depending on the relaxation parameter.

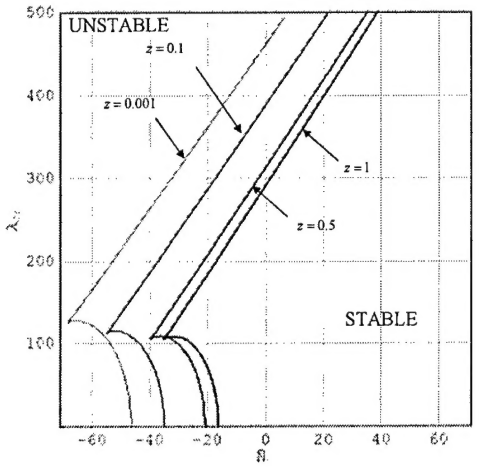

Figure 3 Boundaries of panel flutter on the $\lambda - \bar{N}_0$ *plane for different values of relaxation parameter and for* $\zeta = 0.001$; $\hat{\zeta} = 0.1$.

The panel experiences flutter above the critical value of dynamic pressure depending on the relaxation parameter. The inclusion of nonlinearities in equations (6) causes the flutter to achieve a limit cycle. However, as shown by the relaxation time history record in Figure 8(a), the panel response experiences nonstationary limit cycle oscillations as the dynamic pressure exceeds its critical value. For dynamic pressure values that exceed the critical value of the clamped condition, the panel experiences unsteady LCO during the relaxation process as shown in Figure 8(b). It is seen that the amplitude of LCO increases with time as the panel boundary conditions change from clamped to near simple support conditions. In all time history records the LCO does not have zero mean value due to the pressure differential.

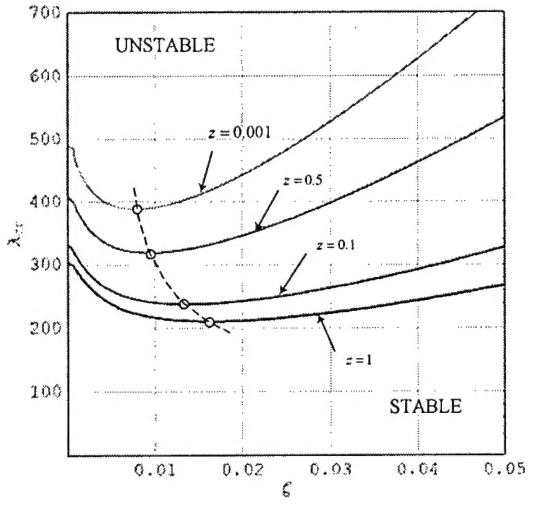

Figure 4 Boundaries of panel flutter on the $\lambda-\zeta$ plane for different values of relaxation parameter and for $\bar{N}_0 = 0.0;\ \hat{\zeta} = 0.1$.

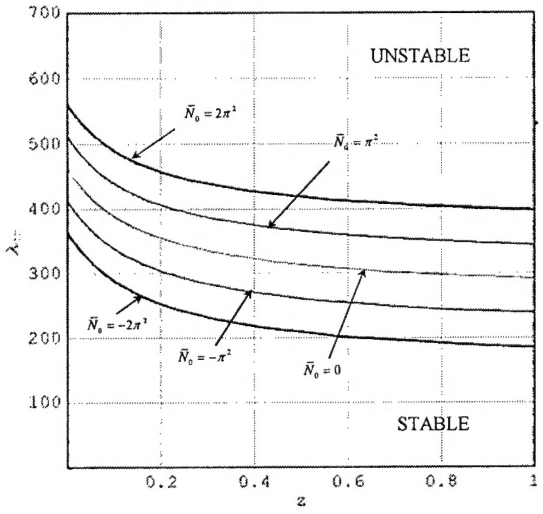

Figure 5 Boundaries of panel flutter on the $\lambda-z$ plane for different values of in-plane load $\bar{N}_0$ and for $\zeta = 0.001;\ \hat{\zeta} = 0.1$.

The FFT and spectrogram plots of the first mode shown in Figure 9 reveal that the frequency content includes one spike at zero frequency, due to the static pressure differential, and a band limited response covering a frequency band that depends on the dynamic pressure. This frequency band reflects the time variation of the panel frequency with time. This is demonstrated by inspecting the corresponding spectrogram. The time evolution of the frequency content represented by the spectrogram demonstrates the correlation between the variation of the frequency with the relaxation process and dynamic pressure.

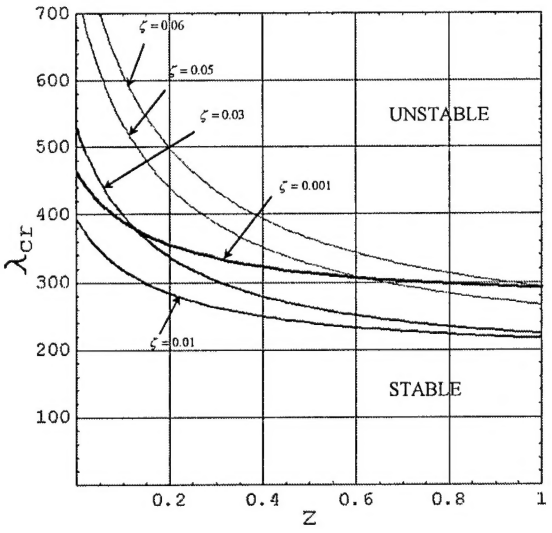

Figure 6 Boundaries of panel flutter on the $\lambda-z$ plane for different values of damping factor showing the reversal effect of damping for $\hat{\zeta} = 0.1, \bar{N}_0 = 0$.

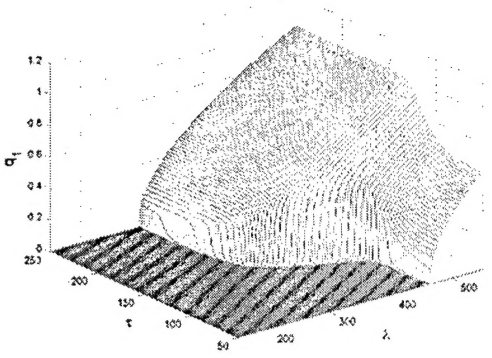

Figure 7 Three-dimensional plots of amplitudes time evolutions and their dependence on dynamic pressure for $\zeta = 0.001,\ \hat{\zeta} = 0.1,\ \bar{p}_0 = 1$, and $N_0 = 0$.

For the case, $\lambda = 500, \zeta = 0.01$, the response frequency increases as the joint passes through relaxation. On the one hand, the relaxation results in a reduction of the panel natural frequency. On the other hand, the nonlinearity of the panel is stiffening and causes an increase in the frequency with the LCO amplitude. It appears that the nonlinearity overcomes the softening effect of

relaxation for the case of Figure 9.

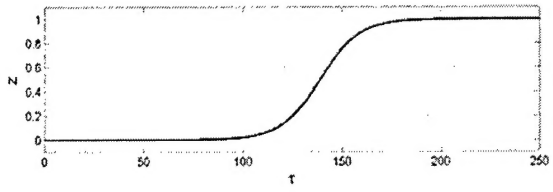

(a)

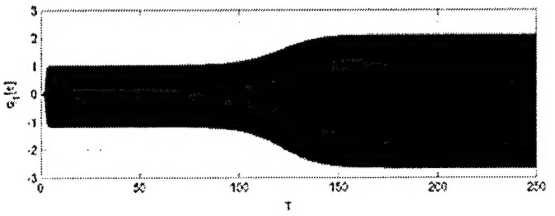

(b)

Figure 8 Time history of the (a) relaxation parameter z ,(b) modal amplitudes for $\bar{p}_0 = 1$

$$\lambda = 500 > \lambda_{cr}, \zeta = 0.01,\ \hat{\zeta} = 0.1,\ \bar{N}_0 = 0$$

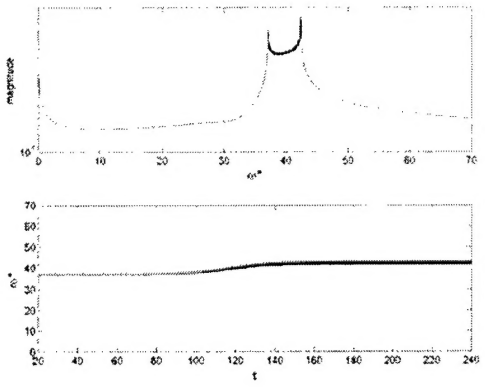

Figure 9 FFT plots and spectrograms for

$$\lambda = 500, \zeta = 0.01,\ \hat{\zeta} = 0.1,\ \bar{N}_0 = 0.$$

2.2 Random Analysis

The panel is exposed to turbulent pressure fluctuations within the boundary-layers. These fluctuations are random and the pressure is characterized by a power spectral density for which empirical expressions can be used, or an assumed Markov field may be introduced. In this section we consider randomness in the in-plane loading only.

In equations (6) the in-plane loading, $\bar{N}_{x0}(\tau)$, will be represented by a mean value superimposed with a random component, $\bar{N}_{x0}(\tau) = \bar{N}_0 + N_x(\tau)$, where $N_x(\tau)$ is independent Gaussian wide-band random processes with zero mean. Owing to the nonstationarity of the panel response it is convenient to carry out Monte Carlo simulation to estimate the response mean squares and stability boundaries.

The dependence of the first mode mean square response on the in-plane power spectral density for zero dynamic pressure is shown in Figure 10 for different values of relaxation parameter, z. It is seen that the bifurcation point for the case of nearly clamped-clamped boundaries ($z = 0.001$) occurs at larger value of in-plane load level than the case of near simply-simply supported panel ($z = 1$). This trend is maintained for any value of dynamic pressure $\lambda < \lambda_{cr}$. For $\lambda > \lambda_{cr}$, the bifurcation point disappears and the panel possesses a non-zero mean square response at zero in-plane level. Monte Carlo simulation was carried out for an ensemble of 250 excitation samples and the response statistics were determined in the time and frequency domains.

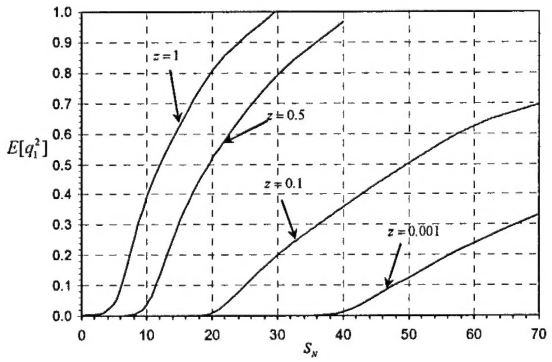

Figure 10 Dependence of first mode mean square response on in-plane power spectral density level for different values of relaxation parameter z, and

$$\zeta = 0.001,\ \hat{\zeta} = 0.1,\ \bar{p}_0 = \bar{N}_0 = 0,\ \lambda = 0.$$

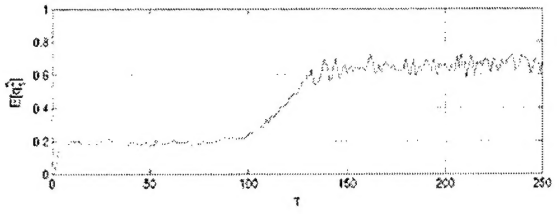

Figure 11 Mean square response of the first mode under in-plane random excitation for $\lambda = 500$,

$$\zeta = 0.001,\ \hat{\zeta} = 0.1,\ \bar{p}_0 = 1, \bar{N}_0 = 0,\ \textit{and}\ S_N = 40$$

Figure 11 shows the time evolution of the mean square response of the first mode. It reveals non-stationarity during the relaxation process. Away from region of relation the mean square response is almost stationary as reflected in the beginning and the end of the time history.

3. CONCLUSIONS

The influence of boundary conditions relaxation on a two-dimensional panel flutter has been studied under deterministic and random conditions. The panel flutter is studied in terms of the first two modes whose eigenvalues are estimated based on the linear modal differential equations. The real value of the eigenvalues determines the critical flutter speed and the relaxation of the boundary conditions reduces the value of the flutter speed. The boundaries of panel flutter are obtained in terms of in-plane load, relaxation parameter, and damping factor. The damping of the panel exhibits a critical value governed by the relaxation parameter, below which the damping has a destabilizing effect and above which it has stabilizing effect. The dependence of the LCO amplitude on dynamic pressure is obtained for different values of relaxation parameter and is found to be bounded between the two limiting cases of simply-supported and clamped-supported boundary conditions. The amplitude time history records reveal an increase in the modal amplitudes after the end of relaxation since the boundary conditions are nearly simply supported. However, the frequency content is governed by the relaxation, geometric nonlinearity, and damping. There is a competition among these three parameters, which causes the frequency content to either increase or decrease with time.

Under random in-plane loading, the stochastic mean square stability boundaries were obtained for dynamic pressures below the critical flutter value. As the dynamic pressure increases, but still below the critical value, the stability region is enlarged because of aerodynamic damping. Above the critical value, the panel modes achieve random LCO whose mean square bifurcates from the critical value of in-plane excitation level, S_N. The time history records display non-stationary random fluctuations during the relaxation process and the scatter is persistent before and after relaxation.

Acknowledgement

This research is supported by the Air Force Office of Scientific Research under grant number F49620-03-1-0229. Dr. Dean Mook is the AFOSR Program Director.

4. REFERENCES

Ibrahim, R. A., Orono, P. O. and Madaboosi, S. R., 1990, Stochastic Flutter of a Panel Subjected to Random In-Plane Forces, Part I: Two Mode Interaction," *AIAA Journal*, Vol. 28, No. 4, pp. 694-702.

Ibrahim, R. A. and Orono, P. O., 1991, Stochastic Nonlinear Flutter of a Panel Subjected to Random In-Plane Forces, *Int. J. Nonlinear Mechanics*, Vol. 26, No. 6, pp./867-883.

Ibrahim, R. A. and C. L. Pettit, 2004, Uncertainties and dynamic problems of bolted joints and other fasteners, *Journal of Sound and Vibration*, in press.

Poiron, B., 1995, Impact of Random Uncertainties on Aircraft Aeroelastic Stability, Proc. Stochastic Structural Dynamics Conference, San Juan, Puerto Rico.

Lindsley, N. J., Beran, P. S., and Pettit, C. L., 2002a, Effects of Uncertainty on Nonlinear Plate Response in Supersonic Flow, 9th AIAA Symp *Multidisciplinary Analysis and Optimization*, Atlanta, GA, Paper 2002-5600.

Lindsley, N. J., Beran, P. S., and Pettit, C. L., 2002b, Effects of Uncertainty on Nonlinear Plate Aeroelastic Response, 43rd AIAA/ASME/ASCE/ AHS /ASCE *Struct Struct Dyn Mater* Conf. Paper No. AIAA 2002-1271.

Ibrahim, R. A., Beloiu, D. M., and Pettit, C. L., 2003, Influence of Boundary Conditions Relaxation on Panel Flutter," Proc. Of the IUTAM Symposium on Chaotic Dynamics and Control Systems Processes in Mechanics, in press.

Qiao, S., Pilipchuk, V. N. and Ibrahim, R. A., 2000, Modeling and simulation of elastic structures with parameter uncertainties and relaxation of joints, *ASME Journal of Vibration and Acoustics, Vol.* 123, No. 1, 2000, pp. 45-52.